Check for updates

Wiley
Journal of Applied Mathematics
Volume 2025, Article ID 5536333, 28 pages
https://doi.org/10.1155/jama/5536333

WILEY

Research Article

Mathematical Modelling of Tumour Treatment With Chemotherapy

F. S. Nyaweni and W. Mbava

Department of Mathematics, Nelson Mandela University, Port Elizabeth, South Africa

Correspondence should be addressed to W. Mbava; willard.mbava@mandela.ac.za

Received 22 October 2024; Revised 15 August 2025; Accepted 3 September 2025

Academic Editor: Yeou Jiann Lim

Copyright © 2025 F. S. Nyaweni and W. Mbava. Journal of Applied Mathematics published by John Wiley & Sons Ltd. This is an open access article under the terms of the Creative Commons Attribution License, which permits use, distribution and reproduction in any medium, provided the original work is properly cited.

In this study, a cancer disease model incorporating dynamics between immune cells and tumour cells, as well as competition between tumour cells and normal cells, was formulated in an attempt to understand the interaction dynamics that govern the complex interplay within the tumour microenvironment. Mathematical analysis has been employed to derive conditions for the boundedness of solutions and to discuss disease thresholds such as the basic reproduction number. Numerical simulations have been conducted, utilising the Runge–Kutta scheme to solve the model. Furthermore, the model was extended to include chemotherapy treatment and reformulated as an optimal control problem. Optimal control techniques have been applied to examine the role of chemotherapy in enhancing tumour cell elimination and minimising adverse effects on immune cells and normal cells. The results indicate that a low concentration of the drug leads to a prolonged period for tumour clearance. Conversely, a higher drug concentration resulted in a quicker tumour clearance, albeit with adverse effects on normal and effector cells. The optimal control identifies when to stop the treatment once the tumour clears. Furthermore, optimal control facilitates the regeneration of normal and immune cells beyond treatment, in contrast to a control scenario. The findings highlight the importance of early detection and careful chemotherapy dosage selection for effective and personalised cancer treatment strategies.

Keywords: chemotherapy; mathematical modelling; optimal control; tumour

1. Introduction

Cancer, characterised by the uncontrolled proliferation of normal cells, presents a formidable global health challenge, with its incidence soaring exponentially in recent years [1]. The International Agency for Research on Cancer (IARC) reports a staggering rise in cancer cases, underscoring the urgent need for intervention. Tragically, the grim statistics reveal a stark reality: 1 out of 11 women and 1 out of 8 men will succumb to cancer during their lifetimes, with over 50 million people estimated to have a history of cancer diagnosis within 5 years [2]. In 2013 alone, the global burden of cancer amounted to 14.9 million diagnoses, accompanied by 196.3 million disability-adjusted life years (DALYs) attributed to the disease. Within Africa, cancer has emerged as a pressing public health concern, necessitating concerted efforts to curb escalating incidence and mortality rates [3]. Alarmingly, projections indicate a 70% surge in cancer cases by 2030, driven by demographic shifts and population ageing [4]. Against the backdrop of coexisting infectious diseases such as Ebola, malaria, AIDS and COVID-19, cancer rates in Africa have surpassed combined figures for malaria, tuberculosis and AIDS, underscoring the imperative of combatting this growing menace [5, 6]. The World Health Organisation reported that, in 2022, approximately 20 million new cancer cases were diagnosed and about 9.7 million people died from the disease [7]. On a national scale, cancer poses a dual threat to South Africa's health and economy, exerting significant economic tolls alongside health repercussions [8]. Recent statistics underscore the magnitude of the challenge, with over 100,000 new cancer cases and nearly 57,000 cancer-related deaths recorded in 2018 alone [9]. Furthermore, cancer transcends mere pathology, manifesting as a diverse group of diseases characterised by aberrant

growth and spread [10]. Early detection of cancer plays a crucial role in improving prognosis and overall survival rates. Detecting cancer at an earlier stage allows for more effective treatment interventions, leading to better outcomes for patients. However, despite advances in medical technology, a significant portion of cancers are still diagnosed at advanced stages, highlighting the ongoing need for improved early detection methods. Additionally, careful selection of chemotherapy dosage is essential in balancing treatment efficacy with minimising toxic side effects. Finding the optimal dosage for each patient is critical for maximising therapeutic benefits whilst minimising adverse reactions. Current approaches to dose selection often lack precision, leading to potential under- or overdosing in certain patient populations. Thus, there is a pressing need for further research and development in both early detection techniques and personalised dosage selection strategies to enhance cancer treatment effectiveness and improve patient outcomes [11–13].

In this context, mathematical models play an essential role as both a theoretical and numerical foundation for understanding the dynamics of various diseases. This is especially pertinent to mathematical studies in oncology, which involve measuring factors such as tumour size and volume (predicting tumour development), enhancing treatment strategies and ultimately fostering progress in cancer research [14]. Numerous studies have introduced mathematical models to investigate cancer treatment methods, including chemotherapy, immunotherapy and stem cell therapy, with an emphasis on different cell populations and their interactions. For instance, Alqudah [15] introduced an autonomous system to model the dynamics of tumour cells, stem cells and effector cells, incorporating an amplification factor to simplify the interactions. Their analysis showed that tumour growth rates during and after treatment were lower due to the stem cell–aided effector cell interactions. The combination of chemotherapy and stem cell therapy was highlighted for improving the quality of life and enhancing treatment outcomes. Song et al. [16] developed a mathematical model incorporating three cell populations: tumour cells, NK cells and cytotoxic T cells (CTLs), along with a drug concentration variable to examine the combined effects of the immune system and chemotherapy on tumour growth. The study identified key parameters relevant to treatment design, demonstrating the role of immune cells and chemotherapy in reducing tumour burden. However, the model is constrained by several limitations, including the assumption of a constant chemotherapy input, which does not reflect real-world drug pharmacokinetics. Additionally, it does not account for drug resistance mechanisms or the complexities of drug diffusion and delivery, which are critical for accurately modelling treatment efficacy. The model also simplifies immune interactions by focusing primarily on NK cells, overlooking the broader immune response. These limitations reduce its applicability, as tumour response to treatment is highly dynamic and influenced by multiple factors. Pinho et al. [17] focused on cancer metastasis using a model with six differential equations. Their study identified equilibrium points representing different stages of cancer spread and provided insights into how, without immunity, cancer cells would ultimately dominate and lead to death. They explored local asymptotic stability but found no globally stable points, emphasising the complexity of cancer treatment dynamics. De Pillis and Radunskaya [18] presented a phase-space analysis of tumour growth under immune responses and chemotherapy. Their predator–prey model illustrated the competition between tumour and immune cells for resources, utilising optimal control to minimise tumour populations whilst preserving normal cells. Sweilam et al. [19] introduced a nonlinear fractional-order model for cancer treatment, employing fractional differential equations and two distinct simulation methods to validate their theoretical results. Their comparative study found that a two-step Lagrange interpolation method provided better outcomes than the iterative optimal control method. Lestari et al. [20], on the other hand, developed a predator–prey mathematical model to study the spread of cancer during chemotherapy, focusing on the interactions between effector cells, tumour cells and the chemotherapy drug. Their analysis revealed that the growth rate of cancer cells greatly influences tumour population, and increasing chemotherapy dosage within safe limits can effectively reduce the number of cancer cells. Despite extensive research, the impact of tumour growth on patient well-being is underexplored.

This gap highlights the broader challenge within mathematical oncology, where a significant emphasis is placed on identifying optimal therapy strategies. Optimal control law primarily has the role of designing treatment regimes towards keeping tumour load to a minimum, maintaining healthy and immune cells and using the least drugs [14]. Several studies have aimed at obtaining optimal control strategies to maximise the effectiveness of chemotherapy and immunotherapy from Pontryagin's maximum principle (PMP) and other numerical approaches. Jena et al. [14] used bifurcation analysis to investigate complex dynamical behaviour and proposed optimal control strategies to minimise tumour growth whilst reducing chemotherapy drug usage and associated side effects. Their results indicated that the bifurcation analysis identified regions of stability and where tumour cells may be eradicated. Furthermore, the implementation of optimal control strategy of chemotherapy eradicates tumour cells whilst simultaneously increasing the host and immune cells populations, thereby restoring the system to a healthy state. Dehingia et al. [21] studied the combined effect of optimal controlled chemo–stem cell therapy on a fractional-order cancer model. Their results indicate that stem cell therapy and effector cells combined cannot eradicate tumour cells effectively. However, when chemotherapy is administered under optimal control, the tumour cell population is effectively reduced, whilst the population of normal and effector cells progressively recover as time passes. Salih et al. [22] studied the effect of a psychological scare on the dynamics of the tumour–immune interaction with optimal control strategy. In their findings, through optimal control, they proposed the minimum therapy dosage necessary for eradicating cancer, even in the presence of psychological distress.

4185, 2025, 1, Downloaded from https://onlinelibrary.wiley.com/doi/10.1155/jama/5536333 by South African Medical Research, Wiley Online Library on [24/11/2025]. See the Terms and Conditions (https://onlinelibrary.wiley.com/terms-and-conditions) on Wiley Online Library for rules of use; OA articles are governed by the applicable Creative Commons License

Our model is based on the model proposed by Lestari et al. [20] to bridge that gap by examining how chemotherapy influences the interaction between immune and tumour cells whilst minimising damage to normal cells. Using optimal control theory, the model will optimise chemotherapy application to ensure tumour elimination with minimal adverse effects on the patient. We hypothesise that optimal control can be employed within a tumour–immune–normal cell interaction framework to determine chemotherapy schedules that effectively suppress tumour growth whilst minimising the cytotoxic impact on normal and immune cell populations. Whilst chemotherapy is a key intervention for reducing tumour burden, it also exerts collateral damage on healthy cells involved in immune surveillance and tissue maintenance. We apply the optimal control theory to find treatment protocols to sustain tumour suppression whilst optimising the regeneration of normal tissues and restoration of immune response towards minimising the risk of tumour relapse. This hypothesis is informed by the work of De Pillis and Radunskaya [23], who were emphasising that immune dynamics need to be included to decide treatment protocols. We propose the strategic timing of chemotherapy cessation to augment the natural immunity against residual tumour cells, as has been shown by Emens and Middleton [24]. We also examine whether, without chemotherapy, the immune system can cure tumours on its own [25] and whether immune response with chemotherapy under proper control can result in better therapeutic outcomes [26]. Ultimately, we hypothesise that optimal control offers a viable framework for balancing tumour eradication, immune preservation and normal cell recovery whilst mitigating the risks associated with premature discontinuation of treatment.

The aim of this paper is to develop and analyse a mathematical model of tumour that incorporates the interaction between immune, tumour and normal cells. We will extend the model to include chemotherapy treatment and further investigate the role chemotherapy plays in reducing and eliminating tumour growth as well as the negative effect on normal and immune cells. The overarching goal is to shed light on the efficacy of chemotherapy in tumour suppression whilst mitigating adverse effects on healthy tissues. Through mathematical analysis, numerical simulations and an exploration of optimal control strategies, this research endeavours to inform the development of therapeutic interventions for cancer. By elucidating the complex dynamics underlying tumour growth and treatment response, we aim to pave the way for enhanced treatment strategies and improved outcomes for cancer patients. The organisation of the paper is as follows. In Section 2, we formulate the model that describes the dynamics of tumour cells. In Section 3, we conduct a mathematical analysis of the model to ensure that solutions are feasible and physically realisable. We also identify the equilibrium points in the system and discussed the stability analysis of the model. In Section 4, the optimal control model is formulated and includes the drug intervention. PMP is employed to identify the control strategies and to determine the necessary conditions for the optimal control of the disease. In Section 5, we present the results of the numerical simulations, followed by discussion and conclusion in Section 6.

2. The Model

We first consider the Lestari cancer model [20] without chemotherapy and extend the model by adding an equation of normal cells to incorporate interaction between normal cells, immune cells and tumour cells. Consequently, we analyse a mathematical model that explores the dynamics amongst normal cells, immune cells and tumour cells. In Section 4, even though in Lestari model they considered chemotherapy treatment by varying parameters, we will consider the extended model to include an equation for chemotherapy treatment under optimal control with chemotherapy as a control variable. We now consider a cancer model in which the interactions amongst normal cells, $N(t)$, immune cells, $E(t)$ and tumour cells, $T(t)$, are considered. The normal and tumour cell populations grow logistically, whilst there is a constant recruitment of effector cells. The elements incorporated into the model are described below.

Normal cells grow logistically represented by the term $r_1N(1 - b_1N)$, where r_1 is the growth rate and b_1 represents their carrying capacity. In the presence of tumour cells, normal cell population decline, due to competition for resources between the normal and tumour cells. This decline is modelled by the term $-c_1TN$, where c_1 represents the rate at which tumour cells damage normal cells or the competition term and T represents the population of tumour cells. The immune cell population is subject to constant growth rate, κ, and decline due to natural mortality μE. Furthermore, the presence of tumour cells stimulates immune cell growth which is governed by the Michaelis–Menten growth modelled by the terms, $q(ET/\alpha + T)$, where q represents the level of recruitment of maximum effector cells relative to cancer cells and α represents the steepness coefficient of recruitment curve of effector–immune cells. On the other hand, the presence of tumour cells inhibits the growth of immune cells, and this is modelled by $-\beta ET$. Nonetheless, the growth of the tumour cell population is represented by the logistic term $r_2T(1 - b_2T)$. Here, r_2 represents the intrinsic growth rate of tumour cells, and b_2 represents the carrying capacity. This term reflects that tumour cell population growth is proportional to the available resources until it reaches a maximum capacity. Furthermore, the decrease in the tumour cell population is associated with the parameter of tumour cleanup by effector cells f and is represented by the interaction term $-fET$. On the other hand, the increase in the tumour cell population is also due to their interaction between tumour and normal cells. This interaction involves the conversion of normal cells into tumour cells, represented as c_2TN. Therefore, the extended mathematical model of the tumour treatment with no chemotherapy or drug intervention is given by the following:

$$\frac{dN}{dt} = r_1N(1 - b_1N) - c_1TN, \tag{1a}$$

4185, 2025, 1, Downloaded from https://onlinelibrary.wiley.com/doi/10.1155/jama/5536333 by South African Medical Research, Wiley Online Library on [24/11/2025]. See the Terms and Conditions (https://onlinelibrary.wiley.com/terms-and-conditions) on Wiley Online Library for rules of use; OA articles are governed by the applicable Creative Commons License

$$\frac{dE}{dt} = \kappa + q\frac{ET}{\alpha + T} - \mu E - \beta ET, \tag{1b}$$

$$\frac{dT}{dt} = r_2 T(1 - b_2 T) + c_2 NT - fET, \tag{1c}$$

where $E(0) = E_0 \geq 0, N(0) = N_0 \geq 0, T(0) = T_0 \geq 0$. All parameters and variables in the model are assumed to be nonnegative.

3. Model Analysis

Within this section, we perform a mathematical examination of the model to determine the conditions under which the solutions to the system (1) remain bounded, maintain nonnegativity within the domain, exist uniquely and are stable.

3.1. Boundedness

Lemma 1. *The positive solutions of the system (1) are bounded; that is, the model variables $N(t)$, $E(t)$ and $T(t)$ are bounded for all t.*

Proof 1. From Equation (1a), we obtain

$$\frac{dN}{dt} = r_1 N(1 - b_1 N) - c_1 TN \leq r_1 N(1 - b_1 N).$$

Separating the variables and integrating yields

$$N(t) \leq \frac{Ae^{rt}}{1 + b_1 Ae^{rt}} = \frac{1}{Be^{-rt} + b_1}.$$

We note that $N(t) \leq 1/b_1$ as $t \longrightarrow \infty$. From Equation (1b), we have

$$\frac{dE}{dt} \leq \kappa + q\frac{ET}{\alpha + T} - \mu E.$$

Since $(T/\alpha + T) \leq 1$, then the equation becomes

$$\frac{dE}{dt} \leq \kappa + qE - \mu E.$$

Separating variables and integrating yields

$$E \leq \frac{\kappa}{\mu - q} + Ae^{-(\mu - q)t}.$$

This implies that

$$\lim_{t \longrightarrow \infty} \sup\,(E(t)) \leq \frac{\kappa}{\mu - q},$$

provided that $q \leq \mu$. From Equation (1c), we have

$$\frac{dT}{dt} \leq r_2 T(1 - b_2 T) + c_2 NT.$$

Since $\lim_{t \longrightarrow \infty} \sup\,(N(t)) = 1/b_1$, we have

$$T(t) \leq \frac{DYe^{Yt}}{1 + De^{Yt}},$$

where $r_2 + (c_2/b_1) = Y > 0$ and D represents the constant of integration. Therefore,

$$\lim_{t \longrightarrow \infty} \sup\,(T(t)) \leq Y.$$

□

3.2. Positivity of Solutions. Based on biological findings, the system (1) will be analysed in the following regions: $\Delta = (N, E, T) \in \mathbb{R}^3_+$, where all values of N, E and T will remain positive for all $t \geq 0$, according to Liu et al. [27] and Gurmu et al. [28].

Theorem 1. *Given that the initial conditions of the system (1) are positive, then the solutions of the system remain positive for all $t \geq 0$ and will remain in $\mathbb{R}^3_+$.*

Proof 2. This proof will follow that of Sowole et al. [29]. The positiveness is determined separately for each of the model variables $N(t)$, $E(t)$ and $T(t)$. From Equation (1a),

$$\frac{dN}{dt} = r_1 N(1 - b_1 N) - c_1 TN \geq -c_1 TN.$$

Substituting the upper bound of $T(t) = Y$ (from Lemma 1) and using separation of variables since $N(t) \neq 0$, the differential inequality becomes

$$\frac{dN(t)}{N(t)} \geq -(c_1 Y)dt,$$

with solution

$$N(t) \geq N(0)\,\exp\,(-c_1 Yt).$$

Therefore, this implies that $\lim_{t \longrightarrow \infty} \inf\,(N(t)) \geq 0$. Similarly, from Equation (1b), we have

$$\frac{dE(t)}{\mathrm{d}t} \geq -(\mu + \beta T(t))E(t).$$

Substituting the upper bound of $T(t) = Y$ where $Y = r_2 + (c_2/b_1)$ and integrating yields

$$E(t) \geq E(0)\,\exp\,(-\mu t - \beta Yt) > 0.$$

Therefore, this implies that $\lim_{t \longrightarrow \infty} \inf E(t) \geq 0$.

Also, from Equation (1c), we have

$$\frac{dT}{dt} \geq -fET,$$

4185, 2025, 1, Downloaded from https://onlinelibrary.wiley.com/doi/10.1155/jama/5536333 by South African Medical Research, Wiley Online Library on [24/11/2025]. See the Terms and Conditions (https://onlinelibrary.wiley.com/terms-and-conditions) on Wiley Online Library for rules of use; OA articles are governed by the applicable Creative Commons License

since $E(t) \leq (\kappa/\mu - q)$ gives

$$T(t) \geq T(0) \exp\left(-\frac{\kappa f t}{\mu - q}\right).$$

This implies that $\lim_{t\longrightarrow\infty} \inf T(t) > 0$. Therefore, the variables N, E and T representing the different cell populations in mathematical modelling of tumour treatment with chemotherapy are positive and will remain in $\mathbb{R}^3_+$ for all $t > 0$. □

We use the Picard–Lindelöf theorem in the paper by Coddington and Levinson [30] and Cid [31] to establish and find the existence of the solutions of the model (1). This theorem is also referred to as the Cauchy–Lipschitz theorem that gives the conditions for system to have a unique solution [32–35].

3.3. Existence and Uniqueness of the Solutions of Model

Theorem 2. *Consider the initial value problem*

$$\frac{dY}{dt} = \Phi(t, Y), \quad Y(t_0) = Y_0, \tag{2}$$

where $\Phi : \mathcal{D} \subset \mathbb{R} \times \mathbb{R}^n \longrightarrow \mathbb{R}^n$ *is a continuous function defined on some domain* $\mathcal{D}$ *containing* (t_0, Y_0) *and* $Y(t) = [N(t), E(t), T(t)]^T$. *If* Φ *satisfies the Lipschitz condition in* Y, *for all* (t, Y_1), (t, Y_2) *in* $\mathcal{D}$, *then there exists an interval* $I = [t_0 - \varepsilon, t_0 + \varepsilon]$ *for some* $\varepsilon > 0$ *where the initial value problem (2) has a unique solution* $Y(t)$ *defined on* I.

Proof 3. This proof follows the approach of Padder et al. [36]. We formulate the system (1) as a vector-valued function and let $Y(t) = [N(t), E(t), T(t)]^T$. Thus, the system (1) can be written as $dY/dt = \Phi(t, Y)$, where we define the vector function

$$\Phi(t, Y) = \begin{bmatrix} r_1 N(1 - b_1 N) - c_1 TN \\ \kappa + q\dfrac{ET}{\alpha + T} - \mu E - \beta ET \\ r_2 T(1 - b_2 T) + c_2 NT - fET \end{bmatrix}. \tag{3}$$

The polynomial terms ($r_1 N$, $r_1 b_1 N^2$, $c_1 TN$, μE, βET, $r_2 T$, $r_2 b_2 T^2$, $c_2 NT$ and fET) are smooth and continuous. The rational term $ET/\alpha + T$ is continuous as long as $\alpha + T \neq 0$. Since $\alpha > 0$ and $T \geq 0$, the denominator never vanishes. Thus, $\Phi(t, Y)$ is continuous in t and Y.

In order to verify the Lipschitz condition, we must show that $\Phi(t, Y)$ satisfies

$$\|\Phi(t, Y_1) - \Phi(t, Y_2)\| \leq \eta \|Y_1 - Y_2\|, \tag{4}$$

for some $\eta > 0$ and all Y_1, Y_2 in some region around the initial conditions.

Let $Y_1 = [N_1, E_1, T_1]^T$, $Y_2 = [N_2, E_2, T_2]^T$. For the first equation of (3),

$$\begin{aligned} &|r_1 N_1(1 - b_1 N_1) - c_1 T_1 N_1 - r_1 N_2(1 - b_1 N_2) + c_1 T_2 N_2|, \\ &= \left|r_1(N_1 - N_2) - r_1 b_1\left(N_1^2 - N_2^2\right) - c_1(T_1 N_1 - T_2 N_2)\right|, \\ &\leq r_1|N_1 - N_2| + r_1 b_1|N_1 + N_2| \cdot |N_1 - N_2| + c_1|T_1 N_1 - T_2 N_2|, \\ &\leq r_1|N_1 - N_2| + r_1 b_1(|N_1| + |N_2|)|N_1 - N_2|, \\ &\cdot + c_1(|T_1| \cdot |N_1 - N_2| + |N_2| \cdot |T_1 - T_2|). \end{aligned}$$

Assuming $|N| \leq M_N$ and $|T| \leq M_T$ in a local region, we obtain

$$\leq (r_1 + 2 r_1 b_1 M_N + c_1 M_T)|N_1 - N_2| + c_1 M_N |T_1 - T_2|.$$

For the second equation of (3),

$$\begin{aligned} &\left|q\left(\frac{E_1 T_1}{\alpha + T_1} - \frac{E_2 T_2}{\alpha + T_2}\right) - \mu(E_1 - E_2) - \beta(E_1 T_1 - E_2 T_2)\right|, \\ &\leq q\left|\frac{E_1 T_1}{\alpha + T_1} - \frac{E_2 T_2}{\alpha + T_2}\right| + \mu|E_1 - E_2| + \beta|E_1 T_1 - E_2 T_2|. \end{aligned}$$

For the rational term,

$$\begin{aligned} &\left|\frac{E_1 T_1}{\alpha + T_1} - \frac{E_2 T_2}{\alpha + T_2}\right| \\ &= \left|\frac{E_1 T_1(\alpha + T_2) - E_2 T_2(\alpha + T_1)}{(\alpha + T_1)(\alpha + T_2)}\right|, \\ &= \left|\frac{\alpha(E_1 T_1 - E_2 T_2) + T_1 T_2(E_1 - E_2)}{(\alpha + T_1)(\alpha + T_2)}\right|, \\ &\leq \frac{|\alpha(E_1 T_1 - E_2 T_2) + T_1 T_2(E_1 - E_2)|}{\alpha^2} \ (\text{since } (\alpha + T_1)(\alpha + T_2) \geq \alpha^2), \\ &\leq \frac{\alpha|E_1 T_1 - E_2 T_2| + |T_1 T_2| \cdot |E_1 - E_2|}{\alpha^2} \ (\text{triangle inequality}), \\ &\leq \frac{1}{\alpha^2}(\alpha(|E_1| \cdot |T_1 - T_2| + |T_2| \cdot |E_1 - E_2|) + |T_1 T_2| \cdot |E_1 - E_2|), \\ &\leq \frac{1}{\alpha^2}\left(\alpha M_E |T_1 - T_2| + \alpha M_T |E_1 - E_2| + M_T^2 |E_1 - E_2|\right), \\ &= \frac{1}{\alpha^2}\left(\alpha M_E |T_1 - T_2| + \left(\alpha M_T + M_T^2\right)|E_1 - E_2|\right), \end{aligned}$$

where $|E_i| \leq M_E$, $|T_i| \leq M_T$.

For the β term,

$$\beta|E_1 T_1 - E_2 T_2| \leq \beta M_E |T_1 - T_2| + \beta M_T |E_1 - E_2|.$$

Combining all terms for the second equation,

$$\begin{aligned} &\leq \left(\mu + \frac{q\left(\alpha M_T + M_T^2\right)}{\alpha^2} + \beta M_T\right)|E_1 - E_2| \\ &\cdot + \left(\frac{q\alpha M_E}{\alpha^2} + \beta M_E\right)|T_1 - T_2|. \end{aligned}$$

4185, 2025, 1, Downloaded from https://onlinelibrary.wiley.com/doi/10.1155/jama/5536333 by South African Medical Research, Wiley Online Library on [24/11/2025]. See the Terms and Conditions (https://onlinelibrary.wiley.com/terms-and-conditions) on Wiley Online Library for rules of use; OA articles are governed by the applicable Creative Commons License

For the third equation of (3),

$$\begin{aligned}
&|r_2T_1(1-b_2T_1)+c_2N_1T_1-fE_1T_1-r_2T_2(1-b_2T_2)-c_2N_2T_2\\
&\quad+fE_2T_2|,\le r_2|T_1-T_2|+r_2b_2\left|T_2^2-T_1^2\right|+c_2|N_1T_1-N_2T_2|\\
&\quad+f|E_1T_1-E_2T_2|,\le r_2|T_1-T_2|+r_2b_2\cdot 2M_T|T_1-T_2|\\
&\quad+c_2(|N_1|\cdot|T_1-T_2|+|T_2|\cdot|N_1-N_2|)+f(M_E|T_1-T_2|\\
&\quad+M_T|E_1-E_2|),\le r_2|T_1-T_2|+2r_2b_2M_T|T_1-T_2|\\
&\quad+c_2(M_N|T_1-T_2|+M_T|N_1-N_2|)\quad(\text{using }|N_i|\le M_N)\\
&\quad+f(M_E|T_1-T_2|+M_T|E_1-E_2|),=(r_2+2r_2b_2M_T+c_2M_N\\
&\quad+fM_E)|T_1-T_2|+c_2M_T|N_1-N_2|+fM_T|E_1-E_2|.
\end{aligned}$$

Combining all components in the norm $\|Y_1-Y_2\|=|N_1-N_2|+|E_1-E_2|+|T_1-T_2|$, we obtain

$$\|\Phi(t,Y_1)-\Phi(t,Y_2)\|\le\eta\|Y_1-Y_2\|,$$

where η is the maximum of the coefficients from the linear combinations after summing over all equations. Since $\Phi(t,Y)$ is continuous and satisfies the Lipschitz condition locally, the system (1) has a unique solution $Y(t)$ for any initial condition $(N_0,E_0,T_0)\ge 0$ in some interval containing the given initial time guaranteeing that the model is well-posed. □

3.4. Equilibria. There are four equilibrium points in the system.

1. Tumour-free equilibrium point (ξ_t): This equilibrium point refers to a point when the cancer cell population has been driven to extinction as a result of competition with normal cells and immune cells. The tumour-free equilibrium is given by

$$\xi_t=\left(\hat{N},\hat{E},\hat{T}\right)=\left(\frac{1}{b_1},\frac{\kappa}{\mu},0\right).$$

Achieving this equilibrium is a desirable outcome, as it implies that the tumour cell population has been effectively controlled or eliminated and normal and effector cells are at a stable state.

2. Type 1 dead equilibrium point (ξ_d^1): The existence of a Type 1 dead equilibrium suggests a scenario where the tumour has overcome the normal cells, rendering them unable to recover by the body's natural defences. This equilibrium point is given by

$$\xi_d^1=\left(\check{N},\check{E},\check{T}\right)=\left(0,r_2-r_2b_2\left(\frac{-a_2+\sqrt{-4a_1a_3+a_2^2}}{2a_1f}\right),\frac{-a_2+\sqrt{-4a_1a_3+a_2^2}}{2a_1}\right),$$

where

$$\begin{cases}
a_1=\mu d_1-qd_2+\beta d_2,\\
a_2=r_2b_2\kappa d_3-qd_1-\mu d_1-\beta d_1+\mu\alpha d_2-\beta\alpha d_2,\\
a_3=\kappa\alpha d_3-\mu\alpha d_1-\beta\alpha d_1.
\end{cases}\tag{5}$$

We can write a_3 as

$$\begin{cases}
a_3=\kappa\alpha d_3-\alpha d_1(\mu+\beta),\\
=\kappa\alpha d_3\left[1-\dfrac{\alpha d_1(\mu+\beta)}{\kappa\alpha d_3}\right],\\
=\kappa[1-\mathscr{R}_{01}],\text{ where }\mathscr{R}_{01}=\dfrac{d_1(\mu+\beta)}{\kappa d_3}.
\end{cases}$$

To ensure positivity of steady state, we derive conditions on a_1, a_3 such that $\sqrt{a_2^2-4a_1a_3}-a_2>0$. Now, $a_1>0$ if $\mu d_1>\beta dqd_2$, $a_2>0$ if $r_2b_2\kappa d_3+\mu\alpha d_2>qd_1+\mu d_1+\beta d_1+\beta\alpha$ and $a_3<0$ if $\kappa\alpha d_3<\mu\alpha d_1+\beta\alpha d_1$.

This equilibrium state might represent a more advanced or aggressive stage of cancer, where the tumour has developed mechanisms to invade the immune system or resists treatment. This could have implications for treatment strategies, as it indicates a potential need for interventions that target the survival and growth of tumour cells. This type of equilibrium point informs healthcare professionals about the potential challenges in treating the cancer and the aggressiveness of the tumour cells.

3. Type 2 dead equilibrium point (ξ_d^2): This equilibrium point is defined as one in which both normal cells and tumour cells have been destroyed, Mufudza et al. [37]. The Type 2 dead equilibrium point becomes

$$\xi_d^2=\left(\tilde{N},\tilde{E},\tilde{T}\right)=\left(0,\frac{\kappa}{\mu},0\right).$$

The growth rate of the effector cells leads to the decline of both normal and tumour cell populations. Since $\kappa>0$ and $\mu>0$, all the solutions in the Type 2 dead equilibrium point are all in the feasible region. This scenario suggests an effective immune response or treatment strategy that not only eliminates tumour cells but also impacts normal cells, potential due to collateral damage or a strong immune reaction. This equilibrium signifies a scenario where the treatment or immune response has successfully eliminated both the cancerous and healthy cells, achieving a state of equilibrium where no viable cells remain. However, the complete destruction of normal cells may have adverse effects on overall health of the individual. Therefore, in clinical practice, a balance must be struck between eliminating tumour cells and minimising harm to healthy tissues.

4. Coexisting equilibrium point (ξ_c): This equilibrium point represents a scenario where the normal, effector and tumour cells are in a balanced state, coexisting

4185, 2025, 1, Downloaded from https://onlinelibrary.wiley.com/doi/10.1155/jama/5536333 by South African Medical Research, Wiley Online Library on [24/11/2025]. See the Terms and Conditions (https://onlinelibrary.wiley.com/terms-and-conditions) on Wiley Online Library for rules of use; OA articles are governed by the applicable Creative Commons License

without any population dominating the others. This could represent a situation where the immune system is effectively controlling the growth of tumour cells, and a dynamic equilibrium is reached. The endemic equilibrium point becomes

System (1) admits a coexistence equilibrium point in which T^* is a positive solution of the cubic equation:

$$a_6T^3 + a_5T^2 + a_4T + a_0 = 0. \tag{6}$$

Solving this yields the positive root as

$$T^* = -\frac{a_5}{3a_6} - \frac{\sqrt[3]{2}\left(3a_4a_6 - a_5^2\right)}{3a_6\sqrt[3]{9a_4a_6a_5 - 2a_5^3 - 27a_0a_6^2 + \sqrt{4\left(3a_4a_6 - a_5^2\right)^3 + \left(-2a_5^3 + 9a_4a_6a_5 - 27a_0a_6^2\right)^2}}} + \frac{\sqrt[3]{-2a_5^3 + 9a_4a_6a_5 - 27a_0a_6^2 + \sqrt{4\left(3a_4a_6 - a_5^2\right)^3 + \left(-2a_5^3 + 9a_4a_6a_5 - 27a_0a_6^2\right)^2}}}{3\sqrt[3]{2}a_6},$$

$$\xi_c = (N^*, E^*, T^*) = \left(\frac{r_1 - c_1\phi_1 + c_1\phi_2 - c_1\phi_3}{b_1}, \frac{d_4 - d_5\phi_1 + d_5\phi_2 - d_5\phi_3}{d_6}, -\phi_1 - \phi_2 + \phi_3\right).$$

where

$$\begin{cases} a_6 = \beta d_6, \\ a_5 = \mu d_5 + \beta d_5 + \beta\alpha d_5 - \beta d_1 - q d_5, \\ a_4 = \mu\alpha d_5 + \beta\alpha d_5 - \beta\alpha d_4 - \mu d_4 + q d_4 + \kappa d_6, \\ a_0 = \kappa\alpha d_3 - \mu\alpha d_4 - \beta\alpha d_1. \end{cases} \tag{7}$$

T^* can be written as $T^* = -\phi_1 - \phi_2 + \phi_3$, where

$$\begin{cases} \phi_1 = \dfrac{a_5}{3a_6}, \\ \phi_2 = \dfrac{\sqrt[3]{2}\left(3a_4a_6 - a_5^2\right)}{3a_6\sqrt[3]{-2a_5^3 + 9a_4a_6a_5 - 27a_0a_6^2 + \sqrt{4\left(3a_4a_6 - a_5^2\right)^3 + \left(-2a_5^3 + 9a_4a_6a_5 - 27a_0a_6^2\right)^2}}}, \\ \phi_3 = \dfrac{\sqrt[3]{-2a_5^3 + 9a_4a_6a_5 - 27a_0a_6^2 + \sqrt{4\left(3a_4a_6 - a_5^2\right)^3 + \left(-2a_5^3 + 9a_4a_6a_5 - 27a_0a_6^2\right)^2}}}{3\sqrt[3]{2}a_6}. \end{cases}$$

T^* is positive if $\phi_1 + \phi_2 < \phi_3$. Therefore, if $\phi_1 > 0$, both a_5 and a_6 need to have the same sign. For $\phi_2 > 0$, we need $3a_4a_6 - a_5^2 > 0$ and a_6 to have the same sign. For $\phi_3 > 0$, the expression inside the cube root needs to be positive and a_6 to have the same sign. E^* and N^* are obtained from T^*. We have $E^* = (d_4 - d_5T^*)/d_6$ which simplifies to $E^* = (d_4 - d_5\phi_1 + d_5\phi_2 - d_5\phi_3)/d_6$ and $E^* > 0$ if $d_4 - d_5\phi_1 + d_5\phi_2 - d_5\phi_3 > 0$. N^* is given by $N^* = (r_1 - c_1T^*)/b_1$ which simplifies to $N^* = (r_1 - c_1\phi_1 + c_1\phi_2 - c_1\phi_3)/b_1$ and $N^* > 0$, if $r_1 - c_1\phi_1 + c_1\phi_2 - c_1\phi_3 > 0$.

Therefore, the coexisting equilibrium point of the system is given by $\xi_c = (N^*, E^*, T^*) = ((r_1 - c_1\phi_1 + c_1\phi_2 - c_1\phi_3)/b_1, (d_4 - d_5\phi_1 + d_5\phi_2 - d_5\phi_3)/d_6, -\phi_1 - \phi_2 + \phi_3)$.

This equilibrium implies that the tumour cells are being held in check by the immune response, preventing uncontrolled proliferation.

3.5. The Basic Reproductive Number. The basic reproductive number, $\mathscr{R}_0$, can be defined as the average number of secondary infections caused by a single infected individual in a completely susceptible population. In this study, $\mathscr{R}_0$ is

4185, 2025, 1, Downloaded from https://onlinelibrary.wiley.com/doi/10.1155/jama/5536333 by South African Medical Research, Wiley Online Library on [24/11/2025]. See the Terms and Conditions (https://onlinelibrary.wiley.com/terms-and-conditions) on Wiley Online Library for rules of use; OA articles are governed by the applicable Creative Commons License

determined using the next-generation matrix approach as outlined in Van Den Driessche and Watmough's work [38]. To determine $\mathscr{R}_0$ system, we use the new rearranged system showing infection classes below:

$$\begin{aligned}\frac{dT}{dt} &= r_2T(1-b_2T)+c_2NT-fET,\\ \frac{dE}{dt} &= \kappa+q\frac{ET}{\alpha+T}-\mu E-\beta ET.\end{aligned} \tag{8}$$

We generate matrices F and V as

$$F=\begin{bmatrix} r_2T(1-b_2T)+c_2NT-fET \\ 0 \end{bmatrix}, V=\begin{bmatrix} fET \\ -\kappa-\dfrac{qET}{\alpha+T}+\mu E+\beta ET \end{bmatrix}. \tag{9}$$

From (9), the rate of appearance of new metastasis of tumour in compartment is computed by taking the partial respective of F with respect to T and E which is given as follows:

$$\mathscr{F}=\begin{bmatrix} r_2-2r_2b_2T+c_2N-fE & -\mathrm{FT} \\ 0 & 0 \end{bmatrix}. \tag{10}$$

The rate of transfer or transmission of the metastasis of tumour into compartments is computed by taking the partial respective of matrix V with respect to T and E which is given as follows:

$$\mathscr{V}=\begin{bmatrix} fE & \mathrm{fT} \\ -\dfrac{\alpha qE}{(\alpha+T)^2}+\beta E & \dfrac{qT}{\alpha+T}+\mu+\beta T \end{bmatrix}. \tag{11}$$

The matrices $\mathscr{F}$ and $\mathscr{V}$ are evaluated at tumour-free equilibrium point where $(N,E,T)=(1/b_1,\kappa/\mu,0)$ to become

$$\mathscr{F}=\begin{bmatrix} r_2+\dfrac{c_2}{b_1}-\dfrac{fk}{u} & 0 \\ 0 & 0 \end{bmatrix} \quad \text{and} \quad \mathscr{V}=\begin{bmatrix} \dfrac{\kappa f}{\mu} & 0 \\ \dfrac{-q\kappa}{\alpha\mu}+\dfrac{\beta\kappa}{\mu} & \mu \end{bmatrix}.$$

Therefore,

$$\mathscr{F}\mathscr{V}^{-1}=\begin{bmatrix} \dfrac{b_1r_2\mu+c_2\mu^2-b_1f\kappa}{b_1f\kappa\mu} & 0 \\ 0 & 0 \end{bmatrix}. \tag{12}$$

Finally, we compute the eigenvalues from $|\mathscr{F}\mathscr{V}^{-1}-\lambda I|=0$ which gives us a characteristics polynomial of

$$p(\lambda)=\lambda^2+\frac{(\kappa fb_1-r_2b_1u-c_2u)\lambda\mu}{f\kappa ub_1}=0. \tag{13}$$

Solving for the eigenvalues gives $\lambda_1=0$ and $\lambda_2=(r_2b_1\mu+c_2\mu-\kappa fb_1)/f\kappa b_1$. Thus, the basic reproductive number, $\mathscr{R}_0$, is the dominant eigenvalue or maximum modulus eigenvalue (spectral radius) of the Jacobian matrix $\mathscr{F}\mathscr{V}^{-1}$ evaluated at tumour-free equilibrium point and is given by

$$\begin{aligned}\mathscr{R}_0 &= \max\left|\mathscr{F}\mathscr{V}^{-1}-\lambda I\right| = \max\left|\mathscr{F}\mathscr{V}^{-1}-\lambda I\right|\\ &= \max\{|\lambda_1|,|\lambda_2|\}=\frac{r_2b_1\mu+c_2\mu-\kappa fb_1}{f\kappa b_1}.\end{aligned} \tag{14}$$

Therefore, if $\mathscr{R}_0=(r_2b_1\mu+c_2\mu-\kappa fb_1)/f\kappa b_1<1$, then the tumour-free equilibrium is stable, and the metastasis of the tumour dies out. Hence, if $\mathscr{R}_0>1$, the tumour-free equilibrium is unstable, and the metastasis of the tumour continues to increase.

3.6. Stability Analysis of the Steady States

3.6.1. Local Asymptotic Stability of Steady States. The local asymptotically stability (LAS) will be discussed using the Jacobian of the system (1) given by

$$J=\begin{bmatrix} r_1-2r_1b_1N-c_1T & 0 & -c_1T \\ 0 & \dfrac{qT}{\alpha+T}-\mu-\beta T & \dfrac{\alpha qE}{(\alpha+T)^2}-\beta E \\ c_2T & \mathrm{fT} & r_2-r_2b_2T+c_2N-fE \end{bmatrix}. \tag{15}$$

Proposition 1. *The tumour-free equilibrium point for the system (1) is locally asymptotically stable if $f\kappa b_1\mu+r_2b_1\mu>c_2\mu$; otherwise, it is unstable.*

Proof 4. At the tumour-free equilibrium point given by $\xi_t=(1/b_1,\kappa/\mu,0)$, the Jacobian matrix (15) becomes

$$J(\xi_t)=\begin{bmatrix} -r_1 & 0 & 0 \\ 0 & -\mu & \dfrac{\kappa(q-\beta\alpha)}{\mu} \\ 0 & 0 & r_2-\dfrac{c_2}{b_1}-f\dfrac{\kappa}{\mu} \end{bmatrix}. \tag{16}$$

The eigenvalues of the matrix are $\lambda_1=-r_1$, $\lambda_2=-\mu$ and $\lambda_3=r_2[1-((c_2/r_2b_1)+(f\kappa/\mu r_2))]=r_2[1-\mathscr{R}_{01}]$.

Therefore, all the eigenvalues are negative, if $\mathscr{R}_{01}>1$. If $\mathscr{R}_{01}>1$, the tumour-free equilibrium is locally asymptotically stable. This implies that the biological system has mechanisms to resist tumour growth and the system will tend to return to a state without tumours even after small disturbances. On the other hand, if $\mathscr{R}_{01}<1$, the equilibrium is unstable, which implies that the system is prone to tumour development and may require external interventions or treatment to prevent uncontrolled tumour growth. □

Proposition 2. *The Type 1 dead equilibrium point for the system (1) is locally asymptotically stable if $\tau_1<0$, $\tau_6<0$ and $\tau_3<0$; otherwise, it is unstable.*

4185, 2025, 1, Downloaded from https://onlinelibrary.wiley.com/doi/10.1155/jama/5536333 by South African Medical Research, Wiley Online Library on [24/11/2025]. See the Terms and Conditions (https://onlinelibrary.wiley.com/terms-and-conditions) on Wiley Online Library for rules of use; OA articles are governed by the applicable Creative Commons License

Proof 5. At Type 1 dead equilibrium point given by

$$\xi_d^1 = \left(\check{N}, \check{E}, \check{T}\right) = \left(0, r_2 - r_2 b_2\left(\frac{-a_2 + \sqrt{-4a_1a_3 + a_2^2}}{2a_1 f}\right), \frac{-a_2 + \sqrt{-4a_1a_3 + a_2^2}}{2a_1}\right),$$

the Jacobian matrix (15) becomes

$$J\left(\xi_d^1\right) = \begin{bmatrix} -\tau_1 & 0 & \tau_2 \\ 0 & \tau_3 & 0 \\ \tau_4 & \tau_5 & \tau_6 \end{bmatrix}, \tag{17}$$

where

$$\begin{cases} \tau_1 = \dfrac{2r_1a_1 + c_1a_2 - c_1\sqrt{-4a_1a_2 + a_2^2}}{2a_1}, \\ \tau_2 = -\dfrac{c_1\left(-a_2 + \sqrt{-4a_1a_2 + a_2^2}\right)}{2a_1}, \\ \tau_3 = r_2 - \dfrac{r_2b_2\left(-a_2 + \sqrt{-4a_1a_2 + a_2^2}\right)}{2a_1} - \dfrac{-a_2 + \sqrt{-4a_1a_2 + a_2^2}}{2a_1}, \\ \tau_4 = \dfrac{\left(-2\alpha a_1 + a_2 - \sqrt{-4a_1a_2 + a_2^2}\right)\beta\left(\left(-a_2 + \sqrt{-4a_1a_2 + a_2^2}\right)/2a_1\right) + 2q\left(\left(-a_2 + \sqrt{-4a_1a_2 + a_2^2}\right)/2a_1\right)a_1 - 2\mu\left(\alpha a_1 - (a_2/2) + \left(\sqrt{-4a_1a_2 + a_2^2}/2\right)\right)}{2\alpha a_1 + \sqrt{-4a_1a_2 + a_2^2} - a_2}, \\ \tau_5 = -\dfrac{f\left(-a_2 + \sqrt{-4a_1a_2 + a_2^2}\right)}{2a_1}, \\ \tau_6 = \dfrac{r_2b_2a_2 - r_2b_2\sqrt{-4a_1a_2 + a_2^2} + 2r_2a_1 + a_2 - \sqrt{-4a_1a_2 + a_2^2}}{2a_1}. \end{cases}$$

The convergence of the model system (1) around the Type 1 dead equilibrium point depends on the eigenvalues of matrix (17). Thus, the characteristic polynomial equation is as follows:

$$p(\lambda) = (\tau_3 - \lambda)\left\{\lambda^2 + (\tau_1 - \tau_6)\lambda - (\tau_1\tau_6 + \tau_2\tau_4)\right\} = 0. \tag{18}$$

Hence, ξ_d^1 is stable, if the conditions of the polynomial $p(\lambda)$, that is, $\tau_3 < 0$, $\tau_1 - \tau_6 > 0$ and $\tau_1\tau_6 + \tau_2\tau_4 > 0$ are satisfied or if they satisfy $\tau_1 > \tau_6$. Hence, ξ_d^1 is locally asymptotically stable if the conditions are satisfied; otherwise, it is unstable. The stable state represents a scenario where treatment or intervention has successfully eliminated normal cells and the system tends to remain in this tumour state. Hence, the unstable state implies that without meeting certain conditions related to parameter values, the system may not maintain the absence of normal cells. This could be relevant in understanding situations where without ongoing treatment or intervention, normal cells could reappear or proliferate. □

Proposition 3. *The Type 2 dead equilibrium point for the system (1) is locally asymptotically stable if $r_1 < 0$ and $r_2\mu < f\kappa$; otherwise, it is unstable.*

Proof 6. At Type 2 dead equilibrium point given by $\xi_d^2 = (\tilde{N}, \tilde{E}, \tilde{T}) = (0, \kappa/\mu, 0)$, the matrix in (15) becomes

$$J\left(\xi_d^2\right) = \begin{bmatrix} r_1 & 0 & 0 \\ 0 & -\mu & \dfrac{\kappa(q-\mu)}{\alpha\mu} \\ 0 & 0 & r_2 - \dfrac{f\kappa}{\mu} \end{bmatrix}, \tag{19}$$

and the eigenvalues are $\lambda_1 = r_1$, $\lambda_2 = -\mu$ and $\lambda_3 = r_2[1 - f\kappa/\mu r^2] = r_2[1 - \mathcal{R}_{02}]$. Therefore, since $r_1 > 0$, the equilibrium point is unstable. Even if it is a tumour-free equilibrium, we cannot have a situation where one survives with immune cells and no normal cells. The instability of the Type 2 dead equilibrium point implies that a state with complete absence of both normal and tumour cells is not biologically feasible in the long term. In practical terms, it indicates that a system without normal cells is not a sustainable state as the growth and survival of immune cells are dependent on the presence of normal cells. □

Proposition 4. *The endemic equilibrium point is locally asymptotically stable if the following conditions are satisfied:*

4185, 2025, 1, Downloaded from https://onlinelibrary.wiley.com/doi/10.1155/jama/5536333 by South African Medical Research, Wiley Online Library on [24/11/2025]. See the Terms and Conditions (https://onlinelibrary.wiley.com/terms-and-conditions) on Wiley Online Library for rules of use; OA articles are governed by the applicable Creative Commons License

1. *$\lambda_1 < 0$, if $36p_2p_1 < 108p_3 + 8p_1^3$ and if*

$$\left(36p_2p_1 - 108p_3 - 8p_1^3 + 12\sqrt{12p_3p_1^3 - 3p_2^2p_1^2 - 54p_2p_1p_3 + 12p_2^3 + 81p_3^2}\right) > 0,$$

considering the positivity of the square root and the condition that $p_2/3 < p_1^2/9$.

2. *λ_2 and λ_3 have negative real parts if $36p_2p_1 > 108p_3 + 8p_1^3$ and if*

$$\left(36p_2p_1 - 108p_3 - 8p_1^3 + 12\sqrt{12p_3p_1^3 - 3p_2^2p_1^2 - 54p_2p_1p_3 + 12p_2^3 + 81p_3^2}\right) > 0,$$

given the positive square root and the condition that $p_2/3 < p_1^2/9$; otherwise, it is unstable.

Proof 7. At the endemic equilibrium point given by

$$\xi_c = (N^*, E^*, T^*) = \left(\frac{r_1 - c_1\phi_1 + c_1\phi_2 - c_1\phi_3}{b_1}, \frac{d_4 - d_5\phi_1 + d_5\phi_2 - d_5\phi_3}{d_6}, -\phi_1 - \phi_2 + \phi_3\right),$$

the Jacobian matrix (15) becomes

$$J(\xi_c) = \begin{bmatrix} l_1 & 0 & l_2 \\ 0 & l_3 & l_4 \\ l_5 & l_6 & l_7 \end{bmatrix}, \tag{20}$$

where

$$\begin{cases} l_1 = r_1 - 2r_1b_1\left[\frac{r_1 - c_1\phi_1 + c_1\phi_2 - c_1\phi_3}{b_1}\right] - c_1(-\phi_1 - \phi_2 + \phi_3), \\ l_2 = -c_1\left(\frac{d_4 - d_5\phi_1 + d_5\phi_2 - d_5\phi_3}{d_6}\right), \\ l_3 = \frac{q(-\phi_1 - \phi_2 + \phi_3)}{\alpha + (d_4 - d_5\phi_1 + d_5\phi_2 - d_5\phi_3/d_6)} - \mu - \lambda\left(\frac{d_4 - d_5\phi_1 + d_5\phi_2 - d_5\phi_3}{d_6}\right), \\ l_4 = \frac{\alpha q((d_4 - d_5\phi_1 + d_5\phi_2 - d_5\phi_3)/d_6)}{(\alpha + (d_4 - d_5\phi_1 + d_5\phi_2 - d_5\phi_3/d_6))^2} - \lambda\left(\frac{d_4 - d_5\phi_1 + d_5\phi_2 - d_5\phi_3}{d_6}\right), l_5 = c_2\left(\frac{d_4 - d_5\phi_1 + d_5\phi_2 - d_5\phi_3}{d_6}\right), \\ l_6 = f\left(\frac{d_4 - d_5\phi_1 + d_5\phi_2 - d_5\phi_3}{d_6}\right), \\ l_7 = r_2 - r_2b_2(-\phi_1 - \phi_2 + \phi_3) + c_2\left(\frac{r_1 - c_1\phi_1 + c_1\phi_2 - c_1\phi_3}{b_1}\right) - f\left(\frac{d_4 - d_5\phi_1 + d_5\phi_2 - d_5\phi_3}{d_6}\right). \end{cases}$$

The corresponding characteristic equation is

$$p(\lambda) = \lambda^3 - (l_1 + l_3 + l_7)\lambda^2 - (-l_3l_1 - l_7l_1 + l_5l_2 - l_7l_3 + l_6l_4)\lambda - l_1l_3l_7 + l_1l_4l_6 + l_2l_3l_5 = 0,$$

which can be written as $p(\lambda) = \lambda^3 - p_1\lambda^2 + p_2\lambda + p_3$ where

$$\begin{cases} p_0 = 1, \\ p_1 = -(l_1 + l_3 + l_7), \\ p_2 = -(-l_3l_1 - l_7l_1 + l_5l_2 - l_7l_3 + l_6l_4), \\ p_3 = -l_1l_3l_7 + l_1l_4l_6 + l_2l_3l_5. \end{cases}$$

Therefore, λ_1, λ_2 and λ_3 are negative or have negative real parts if the following conditions are met:

Thus, the eigenvalues of this characteristic equation is

- $\lambda_1 < 0$, if $36p_2p_1 < 108p_3 + 8p_1^3$ and if

$$\left(36p_2p_1 - 108p_3 - 8p_1^3 + 12\sqrt{12p_3p_1^3 - 3p_2^2p_1^2 - 54p_2p_1p_3 + 12p_2^3 + 81p_3^2}\right) > 0,$$

considering the positivity of the square root and the condition that $p_2/3 < p_1^2/9$.

- λ_2 and λ_3 have negative real parts if $36p_2p_1 > 108p_3 + 8p_1^3$ and if

$$\left(36p_2p_1 - 108p_3 - 8p_1^3 + 12\sqrt{12p_3p_1^3 - 3p_2^2p_1^2 - 54p_2p_1p_3 + 12p_2^3 + 81p_3^2}\right) > 0,$$

given the positive square root and the condition that $p_2/3 < p_1^2/9$. □

4185, 2025, 1, Downloaded from https://onlinelibrary.wiley.com/doi/10.1155/jama/5536333 by South African Medical Research, Wiley Online Library on [24/11/2025]. See the Terms and Conditions (https://onlinelibrary.wiley.com/terms-and-conditions) on Wiley Online Library for rules of use; OA articles are governed by the applicable Creative Commons License

$$\lambda_1 = \frac{\left(36p_2p_1 - 108p_3 - 8p_1^3 + 12\sqrt{12p_3p_1^3 - 3p_2^2p_1^2 - 54p_2p_1p_3 + 12p_2^3 + 81p_3^2}\right)^{1/3}}{6} - \frac{6\left(p_2/3 - p_1^2/9\right)}{\left(36p_2p_1 - 108p_3 - 8p_1^3 + 12\sqrt{12p_3p_1^3 - 3p_2^2p_1^2 - 54p_2p_1p_3 + 12p_2^3 + 81p_3^2}\right)^{1/3}} - \frac{p_1}{3},$$

$$\lambda_2 = -\frac{\left(36p_2p_1 - 108p_3 - 8p_1^3 + 12\sqrt{12p_3p_1^3 - 3p_2^2p_1^2 - 54p_2p_1p_3 + 12p_2^3 + 81p_3^2}\right)^{1/3}}{12} + \frac{3\left(p_2/3 - p_1^2/9\right)}{\left(36p_2p_1 - 108p_3 - 8p_1^3 + 12\sqrt{12p_3p_1^3 - 3p_2^2p_1^2 - 54p_2p_1p_3 + 12p_2^3 + 81p_3^2}\right)^{1/3}} - \frac{p_1}{3},$$

$$\frac{-1}{2}\left(I\sqrt{3}\left(\frac{\left(36p_2p_1 - 108p_3 - 8p_1^3 + 12\sqrt{12p_3p_1^3 - 3p_2^2p_1^2 - 54p_2p_1p_3 + 12p_2^3 + 81p_3^2}\right)^{1/3}}{6} \frac{6\left(p_2/3 - p_1^2/9\right)}{\left(36p_2p_1 - 108p_3 - 8p_1^3 + 12\sqrt{12p_3p_1^3 - 3p_2^2p_1^2 - 54p_2p_1p_3 + 12p_2^3 + 81p_3^2}\right)^{1/3}}\right),$$

$$\lambda_3 = -\frac{\left(36p_2p_1 - 108p_3 - 8p_1^3 + 12\sqrt{12p_3p_1^3 - 3p_2^2p_1^2 - 54p_2p_1p_3 + 12p_2^3 + 81p_3^2}\right)^{1/3}}{12} + \frac{3\left(p_2/3 - p_1^2/9\right)}{\left(36p_2p_1 - 108p_3 - 8p_1^3 + 12\sqrt{12p_3p_1^3 - 3p_2^2p_1^2 - 54p_2p_1p_3 + 12p_2^3 + 81p_3^2}\right)^{1/3}} \left\{-\frac{p_1}{3} - \frac{I\sqrt{3}\left(\left(36p_2p_1 - 108p_3 - 8p_1^3 + 12\sqrt{12p_3p_1^3 - 3p_2^2p_1^2 - 54p_2p_1p_3 + 12p_2^3 + 81p_3^2}\right)^{1/3}/6\right)}{\left(36p_2p_1 - 108p_3 - 8p_1^3 + 12\sqrt{12p_3p_1^3 - 3p_2^2p_1^2 - 54p_2p_1p_3 + 12p_2^3 + 81p_3^2}\right)^{1/3}}.\right.$$

3.6.2. Global Asymptotic Stability (GAS) of Steady States. In order to discuss the GAS of the tumour-free equilibrium, we are going to invoke the use of Castillo-Chavez method described by Castillo-Chavez et al. [39].

Theorem 3. *The tumour-free equilibrium is globally stable if the following conditions are met:*

- *H1* : $d\mathbf{X}/dt = F(\mathbf{X}, 0)$*, the Jacobian matrix at* ξ_t *is*

$$J_F(\mathbf{X}, 0) = \begin{bmatrix} r_1 - 2r_1b_1N & 0 \\ 0 & -\mu \end{bmatrix}. \tag{21}$$

- *H2* : $G(\mathbf{X}, \mathbf{Z}) = \mathbf{A}\mathbf{Z} - G^*(\mathbf{X}, \mathbf{Z})$ *with* $\mathbf{A} = r_2$*, which is an M-matrix, and* $\mathbf{A}$ *is a* 1×1 *matrix which is positive and* $G^*(\mathbf{X}, \mathbf{Z})$ *is nonnegative in* $\mathbb{R}^3_+$*; otherwise, it is unstable.*

Proof 8. The global stability of the equilibrium point is written as

$$\frac{d\mathbf{X}}{dt} = F(\mathbf{X}, \mathbf{Z}), \tag{22}$$

$$\frac{d\mathbf{Z}}{dt} = G(\mathbf{X}, \mathbf{Z}), \tag{23}$$

where $\mathbf{X} = (N, E)^T$ represents uninfected compartments and $\mathbf{Z} = T$ represents the infected compartment.

Let $\xi_t = (\widehat{N}, \widehat{E}, \widehat{T}) = (1/b_1, \kappa/\mu, 0)$, which denote the tumour-free equilibrium of the system (1). For $\mathbf{X}$ to be globally asymptotically stable, the following conditions $H1$ and $H2$ must be satisfied.

- $H1$. $d\mathbf{X}/dt = F(\mathbf{X}, 0)$ is GAS.

4185, 2025, 1, Downloaded from https://onlinelibrary.wiley.com/doi/10.1155/jama/5536333 by South African Medical Research, Wiley Online Library on [24/11/2025]. See the Terms and Conditions (https://onlinelibrary.wiley.com/terms-and-conditions) on Wiley Online Library for rules of use; OA articles are governed by the applicable Creative Commons License

- $H2$. $G(\mathbf{X},\mathbf{Z}) = \mathbf{AZ} - G^*(\mathbf{X},\mathbf{Z})$, $G(\mathbf{X},\mathbf{Z}) \geq 0$ for $(\mathbf{X},\mathbf{Z}) \in \mathbb{R}^3_+$ where $\mathbf{A} = D_Z G(\mathbf{X}^*, 0)$ in an M-matrix and $\mathbb{R}^3_+$ is in the region where the model makes biological sense.

In our case,

$$F(\mathbf{X},0) = \begin{bmatrix} r_1 N(1 - b_1 N) \\ \kappa - \mu E \end{bmatrix}. \tag{24}$$

$H1$: To show that $d\mathbf{X}/dt = F(\mathbf{X},0)$ is GAS, we calculate its Jacobian matrix at ξ_t given by

$$J_F(\mathbf{X},0) = \begin{bmatrix} r_1 - 2r_1 b_1 N & 0 \\ 0 & -\mu \end{bmatrix}. \tag{25}$$

Then, substituting the tumour-free equilibrium point ξ_t gives the following matrix:

$$J_F(\mathbf{X},0) = \begin{bmatrix} -r_1 & 0 \\ 0 & -\mu \end{bmatrix}. \tag{26}$$

Since the diagonal matrix has negative elements, the corresponding eigenvalues have negative real parts, and hence$d\mathbf{X}/dt = F(\mathbf{X},0)$is globally asymptotically stable.

H_2: To show that $G(\mathbf{X},\mathbf{Z}) = \mathbf{AZ} - G^*(\mathbf{X},\mathbf{Z})$ with $\mathbf{A} = D_Z G(\xi_t, 0)$ is an M-matrix, we need to calculate the derivative of $G(\mathbf{X},\mathbf{Z})$ with respect to $\mathbf{Z}$ and evaluate it at $(\xi_t, 0)$:

$$D_Z G(\mathbf{X},\mathbf{Z}) = r_2(1 - b_2 Z) + c_2 \widehat{N} - f\widehat{E}. \tag{27}$$

Evaluating this at $(\xi_t, 0)$, we get $D_Z G(\xi_t, 0) = r_2$, which is positive. Next, we evaluate $G^*(\mathbf{X},\mathbf{Z})$ at $(\xi_t, 0)$:

$$G^*(\xi_t, 0) = r_2 \widehat{T}\left(1 - b_2 \widehat{T}\right) = 0. \tag{28}$$

Hence, by utilising the Castillo-Chavez method and considering the given expression $G(\mathbf{X},\mathbf{Z}) = \mathbf{AZ} - G(\mathbf{X},\mathbf{Z})$, where $\mathbf{A}$ is a positive 1×1 matrix representing r_2, an M-matrix, and $G(\mathbf{X},\mathbf{Z})$ is nonnegative in the domain $\mathbb{R}^3_+$, we can conclude that the tumour-free equilibrium point ξ_t of the system is GAS. This conclusion is based on the fulfilment of both conditions $H1$ and H_2. This global stability of the tumour-free state implies that, under certain conditions and treatment strategies, the system tends to reach and remain in a state where there are no tumour cells present. It also suggests that, in the absence of tumour cells, the immune response and other factors maintain a balanced and healthy state and the system will tend to stay in that state over time. □

Theorem 4. *The endemic equilibrium point is globally asymptotically stable provided the following conditions are met:*

$$r_1 b_1 (1/b_1 + N_c) + c_1 Y > r_1,$$

$$\frac{2}{N_c^2}\left(-r_1 + r_1 b_1\left(\frac{1}{b_1} + N_c\right) + c_1 Y\right)\frac{2}{E_c^2}\left(-q\frac{Y}{\alpha + Y} + \mu + \beta Y\right) > 0,$$

$$\frac{2c_1}{(E_c^2)(N_c^2)}\left(-q\frac{Y}{\alpha + Y} + \mu + \beta Y\right) > \left(\frac{2}{E_c^2}\right)^2,$$

$$\frac{2}{(N_c^2)(T_c^2)}(-r + r_1 b_1 (1/b_1 + N_c) + c_1 Y) \cdot \left(-r_2 - r_2 b_2 (Y + T_c) + \frac{c_2}{b_1} + \frac{f\kappa}{\mu - q}\right) > \left(\frac{2\beta}{N_c^2}\right),$$

otherwise, it is unstable.

Proof 9. Consider the following Lyapunov function about ξ_c

$$W = \left(\frac{N - N_c}{N_c}\right)^2 + \left(\frac{E - E_c}{E_c}\right)^2 + \left(\frac{T - T_c}{T_c}\right)^2.$$

Differentiating on both sides with respect to time, we get

$$\begin{aligned} \frac{dW}{dt} &= \frac{2}{N_c^2}(N - N_c)\frac{dN}{dt} + \frac{2}{N_c^2}(E - E_c)\frac{dE}{dt} + \frac{2}{N_c^2}(T - T_c)\frac{dT}{dt}, \\ &= \frac{2}{N_c^2}(N - N_c)\{r_1 N(1 - b_1 N) - c_1 TN\} \\ &\quad + \frac{2}{E_c^2}(E - E_c)\left\{\kappa + q\frac{ET}{\alpha + T} - \mu E - \beta ET\right\} \\ &\quad + \frac{2}{T_c^2}(T - T_c)\{r_2 T(1 - b_2 T) + c_2 NT - fET\}. \end{aligned}$$

Incorporating the above terms in dW/dt, we get

$$\begin{aligned} \frac{dW}{dt} &= \frac{2}{N_c}(N - N_c)\{(r_1 N(1 - b_1 N) - c_1 TN) - (r_1 N_c(1 - b_1 N_c) - c_1 T_c N_c)\}, \\ &= \frac{2}{E_c^2}(E - E_c)\left\{\left(\kappa + q\frac{ET}{\alpha + T} - \mu E - \beta ET\right) - \left(\kappa + q\frac{E_c T_c}{\alpha + T_c} - \mu E_c - \beta E_c T_c\right)\right\} \\ &\quad + \frac{2}{T_c^2}(T - T_c)\{(r_2 T(1 - b_2 T) + c_2 NT - fET) - (r_2 T_c(1 - b_2 T_c) + c_2 N_c T_c - fE_c T_c)\}. \end{aligned}$$

Collecting and cancelling terms yield

$$\begin{aligned} \frac{dW}{dt} &= \frac{2}{N_c}(N - N_c)\left(r_1(N - N_c) - r_1 b_1\left(N^2 - {N_c}^2\right) - c_1(TN - T_c N_c)\right), \\ &= \frac{2}{E_c^2}(E - E_c)\left(\left(q\frac{ET}{\alpha + T} - \frac{E_c T_c}{\alpha + T_c}\right) - \mu(E - E_c) - \beta(ET - E_c T_c)\right) \\ &\quad + \frac{2}{T_c^2}(E - T_c)\left((r_2(T - T_c) - r_2 b_2\left(T^2 - {T_c}^2\right) + c_2(NT - N_c T_c) - f(ET - E_c T_c)\right). \end{aligned}$$

After performing certain algebraic manipulations, we reach the following results:

4185, 2025, 1, Downloaded from https://onlinelibrary.wiley.com/doi/10.1155/jama/5536333 by South African Medical Research, Wiley Online Library on [24/11/2025]. See the Terms and Conditions (https://onlinelibrary.wiley.com/terms-and-conditions) on Wiley Online Library for rules of use; OA articles are governed by the applicable Creative Commons License

$$\begin{aligned}\frac{dW}{dt} &= \frac{2}{N_c^2}(N-N_c)^2(r_1 - r_1 b_1(N+N_c) - c_1 T) \\ &\quad + \frac{2}{E_c^2}(E-E_c)^2\left(q\frac{T}{\alpha+T} - \mu - \beta T\right) \\ &\quad + (N-N_c)(E-E_c)\times 0 + \frac{2c_1}{N_c}(N-N_c)(T-T_c), \\ &= \frac{2}{T_c^2}(T-T_c)^2(r_2 - r_2 b_2(T+T_c) + c_2 N - fE) \\ &\quad + \frac{2\beta}{E_c}(E-E_c)(T-T_c) + \frac{2c_2}{T_c}(T-T_c)(N-N_c).\end{aligned}$$

dW/dt can now be written as the sum of the quadratic as follows:

$$\begin{aligned}\frac{dW}{dt} &= -d_{11}(N-N_c)^2 + d_{12}(N-N_c)(E-E_c)\times 0 \\ &\quad + d_{13}(N-N_c)(T-T_c) - d_{22}(E-E_c)^2 \\ &\quad - 2d_{23}(E-E_c)(T-T_c) - d_{33}(T-T_c)^2 \\ &\quad + 2d_{32}(T-T_c)(N-N_c), = -X^T D X,\end{aligned}$$

where $X^T = (N-N_c), (E-E_c), (T-T_c)$ and D is a symmetric matrix given by

$$D = \begin{bmatrix} d_{11} & 0 & d_{13} \\ 0 & d_{22} & d_{23} \\ a_{31} & d_{32} & d_{33} \end{bmatrix},$$

where

$$\begin{cases} d_{11} = \dfrac{2}{N_c^2}(-r_1 + r_1 b_1(N+N_c) + c_1 T), \\ d_{13} = d_{31} = -\dfrac{2c_1}{N_c^2}, \\ d_{22} = \dfrac{2}{E_c^2}\left(-q\dfrac{T}{\alpha+T} + \mu + \beta T\right), \\ d_{23} = a_{32} = -\dfrac{2\beta}{E_c^2}, \\ d_{33} = \dfrac{2}{T_c^2}(-r_2 - r_2 b_2(T+T_c) + c_2 N + fE). \end{cases}$$

Then, $dW/dt < 0$ if the matrix D is positive definite, that is, if all the principal minors of D are positive.

The first principal minor is given by

$$M_1 = \frac{2}{N_c^2}(-r_1 + r_1 b_1(N+N_c) + c_1 T) > 0.$$

$M_1 > 0$ only if $-r_1 + r_1 b_1(N+N_c) + c_1 T > 0$ since all variables are bounded in the region Ω. Now, substituting the upper bounds of the variables yields

$$-r_1 + r_1 b_1(1/b_1 + N_c) + c_1 Y > 0, r_1 b_1(1/b_1 + N_c) + c_1 Y > r_1,$$

which holds, therefore, $M_1 > 0$. For the second principle minor, repeat the process,

$$M_2 = \begin{vmatrix} d_{11} & 0 \\ 0 & d_{22} \end{vmatrix} > 0,$$
$$d_{11} d_{22} > 0.$$

Since $d_{11} > 0$ from M_1 above, it follows that M_2 is positive if $d_{22} > 0$. Substituting the upper bounds of the variables, then $d_{22} > 0$ if

$$\frac{2}{N_c^2}\left(-r_1 + r_1 b_1\left(\frac{1}{b_1} + N_c\right) + c_1 Y\right)\left(\frac{2}{E_c^2}\left(-q\frac{Y}{\alpha+Y} + \mu + \beta Y\right)\right) > 0.$$

Since the above holds, then $M_2 > 0$. The third principal minor

$$M_3 = \begin{vmatrix} d_{11} & 0 & d_{13} \\ 0 & d_{22} & d_{23} \\ d_{31} & d_{32} & d_{33} \end{vmatrix} = d_{11}\left(d_{22}d_{33} - d_{23}^2\right) - d_{13}d_{22}d_{31} > 0,$$

holds if

$$d_{11}\left(d_{22}d_{33} - d_{23}^2\right) - d_{13}d_{22}d_{31} > 0,$$
$$\Rightarrow d_{11}\left(\frac{d_{22}d_{33}}{2} - d_{23}^2\right) + d_{22}\left(\frac{d_{11}d_{33}}{2} - d_{13}^2\right).$$

Since d_{11} holds from M_1 and d_{22} holds from M_2, then for the above inequality to hold, we need the following inequalities to be positive:

$$\left(\frac{d_{22}d_{33}}{2} - d_{23}^2\right) > 0,$$
$$\left(\frac{d_{11}d_{33}}{2} - d_{13}^2\right) > 0.$$

Since all variables are bounded in the region Ω and now substituting the upper bounds of the variables, the above inequality holds if

$$\left(\frac{d_{22}d_{33}}{2} - d_{23}^2\right) > 0,$$
$$\frac{2c_1}{\left(E_c^2\right)\left(N_c^2\right)}\left(-q\frac{Y}{\alpha+Y} + \mu + \beta Y\right) - \left(\frac{2}{E_c^2}\right)^2 > 0,$$
$$\frac{2c_1}{\left(E_c^2\right)\left(N_c^2\right)}\left(-q\frac{Y}{\alpha+Y} + \mu + \beta Y\right) > \left(\frac{2}{E_c^2}\right)^2,$$

and

4185, 2025, 1, Downloaded from https://onlinelibrary.wiley.com/doi/10.1155/jama/5536333 by South African Medical Research, Wiley Online Library on [24/11/2025]. See the Terms and Conditions (https://onlinelibrary.wiley.com/terms-and-conditions) on Wiley Online Library for rules of use; OA articles are governed by the applicable Creative Commons License

$$\left(\frac{d_{11}d_{33}}{2} - d_{13}^2\right) > 0,$$

$$\frac{2}{(N_c^2)(T_c^2)}(-r + r_1 b_1(1/b_1 + N_c) + c_1 Y)\left(-r_2 - r_2 b_2(Y + T_c) + \frac{c_2}{b_1} + \frac{f\kappa}{\mu - q}\right) - \left(\frac{2\beta}{N_c^2}\right) > 0,$$

$$\frac{2}{(N_c^2)(T_c^2)}(-r + r_1 b_1(1/b_1 + N_c) + c_1 Y)\left(-r_2 - r_2 b_2(Y + T_c) + \frac{c_2}{b_1} + \frac{f\kappa}{\mu - q}\right) > \left(\frac{2\beta}{N_c^2}\right).$$

Then, $M_3 > 0$ if the following holds

$$\frac{2c_1}{(E_c^2)(N_c^2)}\left(-q\frac{Y}{\alpha + Y} + \mu + \beta Y\right) > \left(\frac{2}{E_c^2}\right)^2,$$

$$\frac{2}{(N_c^2)(T_c^2)}(-r + r_1 b_1(1/b_1 + N_c) + c_1 Y)\left(-r_2 - r_2 b_2(Y + T_c) + \frac{c_2}{b_1} + \frac{f\kappa}{\mu - q}\right) > \left(\frac{2\beta}{N_c^2}\right).$$

Then, $M_3 > 0$ provided the conditions hold. So the matrix D is positive definite if all the inequalities are satisfied. Therefore, the coexisting equilibrium point ξ_c satisfies all the conditions of the Lyapunov stability theorem, and it is stable. □

The GAS of the endemic equilibrium implies that, under specified conditions, the disease persists in the long term. The population of normal and tumour cells reaches a stable coexistence, and the system does not end to move away from this state over time. This could correspond to a chronic state of the disease, where there is an ongoing presence of both normal and tumour cells and the system reaches a stable balance between the two.

Theorem 5. *The Type 1 dead equilibrium point is globally asymptotically stable in Ω, if the following conditions hold*

$$\mu + \beta Y > q\frac{Y}{\alpha + Y},$$

$$r_2 b_2(Y + \check{T}) + f\frac{\kappa}{\mu - q} > r_2 + c_2\frac{1}{b_1},$$

$$\frac{1}{2}\left(-r_2 + r_2 b_2(Y + \check{T}) - \frac{c_2}{b_1} + \frac{f\kappa}{\mu - q}\right)\left(-r_1 + r_1 b_1(1/b_1 + \check{N}) + c_1 Y\right) > \left(-\frac{2c_2}{Y} - 2c_1\right)^2,$$

$$\frac{1}{\check{E}^2}\left(-q\frac{Y}{\alpha + Y} + \mu + \beta Y\right)\left(-r_1 + r_1 b_1(1/b_1 + \check{N}) + c_1 Y\right) > \left(-\frac{q\alpha}{\check{E}(\alpha + T)(\alpha + \check{T})} + \frac{\beta}{\check{E}}\right),$$

otherwise, it is unstable.

Proof 10. Now, we will show the equilibrium point

$$\xi_d^1 = \left(\check{N}, \check{E}, \check{T}\right) = \left(0, r_2 - r_2 b_2\left(\frac{-a_2 + \sqrt{-4a_1 a_3 + a_2^2}}{2a_1 f}\right), \frac{-a_2 + \sqrt{-4a_1 a_3 + a_2^2}}{2a_1}\right)$$

is globally stable by constructing a Lyapunov function, which described the total eradication of normal cell. We first define a Lyapunov function of the model as

$$W = \left(\frac{E - \check{E}^2}{\check{E}}\right) + \left(\frac{T - \check{T}^2}{\check{T}}\right) + \left(N - \check{N}\right)^2.$$

Clearly, it is observable that $W(\xi_d^1) = 0$ and $W(\xi) > 0$ for all $\xi \neq \xi_d^1$ within the net-plane that encompasses the equilibrium point ξ_d^1. This establishes it as a Lyapunov function. Subsequently, differentiating both sides with respect to time produces

$$\begin{aligned}\frac{dW}{dt} &= \frac{2}{\check{E}^2}\left(E - \check{E}\right)\frac{dE}{dt} + \frac{2}{\check{T}^2}\left(T - \check{T}\right)\frac{dT}{dt} + 2\left(N - \check{N}\right),\\ &= \frac{2}{\check{E}^2}\left(E - \check{E}\right)\left(\kappa + q\frac{ET}{\alpha + T} - \mu E - \beta ET\right)\\ &\quad + \frac{2}{\check{T}^2}\left(T - \check{T}\right)(r_2 T(1 - b_2 T) + c_2 NT - fET)\\ &\quad + 2\left(N - \check{N}\right)(r_1 N(1 - b_1 N) - c_1 TN).\end{aligned}$$

The rest of the proof follows the same lines as that of Theorem 4. For dW/dt to be negative definite, the conditions listed in the theorem above must hold. □

The Type 1 dead equilibrium point ξ_d^1 is globally asymptotically stable if the conditions are met, which indicates that the system will stabilise at the dead equilibrium point under these specified conditions, corresponding to a state where the disease or population component is effectively eradicated or at zero. By aligning the proof structure and conditions with those used for the endemic theorem, the similarity between the theorems becomes clearer, showing that the Type 1 dead equilibrium theorem follows a comparable stability analysis process as the endemic equilibrium.

Theorem 6. *The Type 2 dead equilibrium point is globally asymptotically stable in Ω, if the following conditions hold*

$$\mu + \beta Y > q\frac{Y}{\alpha + Y},$$

$$r_2 b_2(Y + \check{T}) + f\frac{\kappa}{\mu - q} > r_2 + c_2\frac{1}{b_1},$$

$$\frac{1}{2}\left(-r_2 + r_2 b_2(Y + \check{T}) - \frac{c_2}{b_1} + \frac{f\kappa}{\mu - q}\right) \cdot \left(-r_1 + r_1 b_1(1/b_1 + \check{N}) + c_1 Y\right) > (2c_2 - 2c_1)^2,$$

$$\frac{1}{\check{E}^2}\left(-q\frac{Y}{\alpha + Y} + \mu + \beta Y\right)\left(-r_1 + r_1 b_1(1/b_1 + \check{N}) + c_1 Y\right) > \left(-\frac{q\alpha}{\check{E}(\alpha + T)(\alpha + \check{T})} + \frac{\beta}{\check{E}}\right),$$

otherwise, it is unstable.

Proof 11. Now, we will show that the equilibrium point $\xi_d^2 = (\check{N}, \check{E}, \check{T}) = (0, \kappa/\mu, 0)$ is globally stable by constructing a Lyapunov function, which described the total eradication

4185, 2025, 1, Downloaded from https://onlinelibrary.wiley.com/doi/10.1155/jama/5536333 by South African Medical Research, Wiley Online Library on [24/11/2025]. See the Terms and Conditions (https://onlinelibrary.wiley.com/terms-and-conditions) on Wiley Online Library for rules of use; OA articles are governed by the applicable Creative Commons License

of normal cell and tumour cells. We first define a Lyapunov function of the model as

$$H = \left(\frac{E-\tilde{E}}{\tilde{E}}\right)^2 + \left(T-\tilde{T}\right)^2 + \left(N-\tilde{N}\right)^2.$$

Clearly, it is observable that $H(\xi_d^1) = 0$ and $H(\xi) > 0$ for all $\xi \neq \xi_d^2$ within the net-plane that encompasses the equilibrium point ξ_d^2. This establishes it as a Lyapunov function. Subsequently, differentiating both sides with respect to time produces

$$\begin{aligned}\frac{dH}{dt} &= 2\left(N-\tilde{N}\right) + \frac{2}{\tilde{E}^2}\left(E-\tilde{E}\right)\frac{dE}{dt} + 2\left(T-\tilde{T}\right),\\ &= \frac{2}{\tilde{E}^2}\left(E-\tilde{E}\right)\left(\kappa + q\frac{ET}{\alpha+T} - \mu E - \beta ET\right)\\ &\quad + 2\left(T-\tilde{T}\right)\left(r_2T(1-b_2T) + c_2NT - fET\right)\\ &\quad + 2\left(N-\tilde{N}\right)\left(r_1N(1-b_1N) - c_1TN\right).\end{aligned}$$

The rest of the proof follows the same lines as that of Theorem 4. For dH/dt to be negative definite, the conditions listed in the above theorem must hold. □

The Type 2 dead equilibrium point ξ_d^2 is globally asymptotically stable if the conditions are met, which indicates that the system will stabilise at the dead equilibrium point under these specified conditions, corresponding to a state where the disease or population component is effectively eradicated or at zero. By aligning the proof structure and conditions with those used for the endemic theorem, the similarity between the theorems becomes clearer, showing that the Type 2 dead equilibrium theorem follows a comparable stability analysis process as the endemic and Type 1 dead equilibrium theorem.

4. The Optimal Control Problem (OCP)

The optimal control technique is a method commonly used to minimise both drug dosage and tumour cell count whilst ensuring patient health. The method considers drug toxicity to all cell types and is aimed at decreasing tumour populations whilst keeping normal and immune cells above a certain threshold. Using optimal control with constraints, we formulate a chemotherapy protocol as an optimisation problem. The goal is to determine the timing of drug administration within a fixed timeframe to minimise tumour cells whilst preserving healthy cell counts.

4.1. Model Extension With Drug Intervention. In this section, the model (1) was extended with introduction of drug intervention. The following elements were incorporated in the formulation of the extended model with chemotherapy:

1. The interaction between immune cells and chemotherapy drugs has an unintentional adverse impact on immune cells, denoted as $-k_EME$, where k_E represents the rate constant associated with adverse impact of chemotherapy drugs on immune cells E and M denotes the concentration of chemotherapy drugs.
2. Within the population of tumour cells, the reduction in tumour cell numbers is caused by their interaction with chemotherapy drugs, which can lead to tumour cell death, represented as $-k_TMT$, where k_T represents the rate constant associated with the reduction in tumour cell numbers caused by their interaction with chemotherapy drugs.
3. Nonetheless, when chemotherapy drugs are introduced externally, they can lead to the elimination of normal cells, expressed as $-k_NMN$, where k_N represents the rate constant associated with the elimination of normal cells (denoted as N in the model) due to the administration of chemotherapy drugs.

Consequently, when chemotherapy drugs are administered from an external source, the concentration of these drugs is given by $W_M(t)$. Subsequently, the concentration of chemotherapy drugs decreases at a rate proportional to the change, with the rate of change in drug concentration over time described by $W_M(t) - \psi M$, where $W_M(t)$ signifies the administered dose and $-\psi$ represents the washout rate. Therefore, the extended mathematical modelling of the tumour treatment with chemotherapy is as follows:

$$\begin{aligned}\frac{dN}{dt} &= r_1N(1-b_1N) - c_1TN - k_NMN,\\ \frac{dE}{dt} &= \kappa + q\frac{ET}{\alpha+T} - \mu E - \beta ET - k_EME,\\ \frac{dT}{dt} &= r_2T(1-b_2T) + c_2NT - fET - k_TMT,\\ \frac{dM}{dt} &= W_M(t) - \psi M,\end{aligned} \tag{29}$$

where $E(0) = E_0 \geq 0$, $N(0) = N_0 \geq 0$, $T(0) = T_0 \geq 0$ and $M(0) = M_0 \geq 0$.

4.2. Extended Model With Chemotherapy Administered Under Optimal Control. In this section, we explored the extended model with chemotherapy administered under optimal control. The emphasis lied in formulating an OCP that guides the administration of chemotherapy to strike a delicate balance-minimising tumour growth whilst mitigating adverse effects on normal and immune cells. Through the application of quadratic control and PMP [40], we established necessary conditions for optimal control, paving the way for a strategic approach to minimise toxic side effects and restrain tumour growth.

4185, 2025, 1, Downloaded from https://onlinelibrary.wiley.com/doi/10.1155/jama/5536333 by South African Medical Research, Wiley Online Library on [24/11/2025]. See the Terms and Conditions (https://onlinelibrary.wiley.com/terms-and-conditions) on Wiley Online Library for rules of use; OA articles are governed by the applicable Creative Commons License

4.2.1. OCP Formulation. The intervention or treatment, denoted by $M(t)$, influences the state $\mathbf{x}(t)$, representing the populations of normal cells, immune cells, tumour cells and drug concentration, denoted as (N, E, T, M). Throughout the patient's treatment, our aim is to ensure that normal and immune cell counts remain above a fixed threshold. To reduce tumour cell population and minimise side effects, we use the system (29) to formulate the OCP. Our objective is to minimise both drug dosage and tumour population. With that, the OCP is given by

$$\text{Minimise}: J(u(t)) = \int_0^{T_f} \left(T(t) + \frac{\varepsilon_u}{2} B u^2(t) \right) dt, \tag{30}$$

subject to

$$\begin{aligned} \frac{dN}{dt} &= r_1 N(1 - b_1 N) - c_1 TN - (1 - u(t))M(t)N, \\ \frac{dE}{dt} &= \kappa + q\frac{ET}{\alpha + T} - \mu E - \beta ET - (1 - u(t))M(t)E, \\ \frac{dT}{dt} &= r_2 T(1 - b_2 T) + c_2 NT - fET - u(t)M(t)T, \\ \frac{dM}{dt} &= u(t)W_M(t) - \Psi M(t). \end{aligned} \tag{31}$$

Here, $E(0) = E_0 \geq 0$, $T(0) = T_0 \geq 0$, $N(0) = N_0 > 0$, $M(0) = M_0 \geq 0$, $0 < u(t) < 1$ and $k_N = k_E = k_T = 1 - u(t)$. The control constraint is defined as $0 < M_z \leq M(t) \leq M_Z$ for $t \in [0, T_f]$, where $u(t)$ is bounded between 0 and 1. We define constants k_N, k_E and k_T as functions of time:

- $k_N = (1 - u(t))$ represents the effect of the control input $u(t)$ on normal cell population N.
- $k_E = (1 - u(t))$ represents the effect of the control input $u(t)$ on immune cell population E.
- $k_T = u(t)$ represents the direct effect of the control input $u(t)$ on tumour cell population T.

The control function $u(t)$, defined as a piece-wise continuous function, determines the magnitude of k_N, k_E and k_T, with $0 \leq u(t) \leq u_{\max} < 1$.

Additionally, $1 - u(t)$ represents the killing effect: When $u(t) = 0$, chemotherapy affects normal and effector cells, with no impact on tumour cells, whilst $u(t) = 1$ implies chemotherapy selectively targets tumour cells without affecting normal or effector cells. This control allows for adjusting drug dosage based on various factors, such as tumour growth rate or patient tolerance to side effects, ensuring effective treatment whilst minimising adverse effects.

4.2.2. Quadratic Control. The objective function (30) employs quadratic control, known for its effectiveness in managing tumours by restraining growth across various sizes whilst minimising toxic side effects. In our mathematical model addressing chemotherapy treatment for tumours, we establish the presence of an optimal control, necessitating an examination of supersolutions as upper bounds.

Upon confirming the bounded nature of the system, we affirm the existence of an optimal control by drawing upon previous research. Utilising Luke's [41] methodology, we assert the presence of an optimal control capable of minimising the objective functional. Notably, supersolutions $(\bar{N}, \bar{E}, \bar{T}, \bar{M})$ consistently surpass actual solutions (N, E, T, M). The system of equations provided below

$$\begin{cases} \dfrac{\partial \bar{N}}{\partial t} = r_1 N, \\ \dfrac{\partial \bar{E}}{\partial t} = \kappa + q\dfrac{ET}{\alpha + T}, \\ \dfrac{\partial \bar{T}}{\partial t} = r_2 T + c_2 NT, \\ \dfrac{\partial \bar{M}}{\partial t} = 1 \end{cases} \tag{32}$$

are bounded on a finite interval. Since the subsolutions are zero, the results show that our system is bounded. Since our system is bounded, our task is then to demonstrate the existence of optimal control, drawing upon insights from the work of Fleming and Rishel [42].

We now characterise the optimal control using the PMP [40]. The constant B is a measure of the relative cost of the interventions over $[0, T_f]$. The OCP is that of finding optimal functions $u^*(t)$ such that

$$J(u^*) = \min_{\Omega} J_1(u(t)),$$

where

$$\Omega = \{u(t): 0 \leq u(t) \leq u_{\max}, t \in [0, T]\}.$$

The Lagrangian of the optimal control is given by

$$L(N, E, T, M, u) = T(t) + \frac{\varepsilon_u}{2} B u^2(t).$$

For the purpose of determining the necessary conditions for optimal control functions using PMP [40], we define the Hamiltonian, $\mathscr{H}$, for the control problem of the system,

$$\mathscr{H} = L(N, E, T, M, u) + \lambda_1 \frac{dN}{dt} + \lambda_2 \frac{dE}{dt} + \lambda_3 \frac{dT}{dt} + \lambda_4 \frac{dM}{dt},$$

where L is the Lagrangian function and where λ_1, λ_2, λ_3 and λ_4 are adjoints variable for states variable N, E, T and M, respectively. Thus,

4185, 2025, 1, Downloaded from https://onlinelibrary.wiley.com/doi/10.1155/jama/5536333 by South African Medical Research, Wiley Online Library on [24/11/2025]. See the Terms and Conditions (https://onlinelibrary.wiley.com/terms-and-conditions) on Wiley Online Library for rules of use; OA articles are governed by the applicable Creative Commons License

$$\mathscr{H}(t) = T(t) + \frac{\varepsilon_u}{2}Bu^2(t) + \lambda_1(r_1N(1-b_1N) - c_1TN - (1-u(t))M(t)N) + \lambda_2\left(\kappa + q\frac{ET}{\alpha+T} - \mu E - \beta ET - (1-u(t))M(t)E\right) + \lambda_3(r_2T(1-b_2T) + c_2NT - fET - u(t)M(t)T) + \lambda_4(u(t)W_M(t) - \Psi M(t)). \tag{33}$$

tem, there exist adjoint variable $\lambda_i = (\lambda_1, \lambda_2, \lambda_3, \lambda_4) \in \mathbb{R}^4$ *such that*

$$\frac{\mathbf{d}\lambda_i}{dt} = -\frac{\partial \mathscr{H}}{\partial x_i}, i \in \{1, 2, 3, 4\},$$

with optimal $x_1 = N$, $x_2 = E$, $x_3 = T$ *and* $x_4 = M$ *that satisfies the following equations:*

$$\frac{d\lambda_1}{dt} = -\frac{\partial \mathscr{H}}{dN} = -\lambda_1(r_1 - 2r_1b_1N^* - c_1T^* - (1-u(t))M^*(t)) - \lambda_3c_2T^*,$$
$$\frac{d\lambda_2}{dt} = -\frac{\partial \mathscr{H}}{dE} = -\lambda_2\left(\frac{qT^*}{\alpha+T^*} - \mu - \beta T^* - (1-u(t))M^*(t)\right) + \lambda_3fT^*,$$
$$\frac{d\lambda_3}{dt} = -\frac{\partial \mathscr{H}}{dT} = -1 - \lambda_2\left(q\frac{E^*}{(\alpha+T^*)^2} - \beta E^*\right) + \lambda_1c_1N^* - \lambda_3(r_2 - 2r_2b_2T^* - fE^* - u(t)M^*(t) + c_2N^*),$$
$$\frac{d\lambda_4}{dt} = -\frac{\partial \mathscr{H}}{dM} = \lambda_1(1-u(t))N^* + \lambda_2(1-u(t))E^* + \lambda_3u(t)T^*.$$

We find a Hamiltonian function that minimises the objective function or cost functional. The PMP is applied to characterise the optimal control u^* in the following way.

Theorem 7. *Given optimal control* u^* *and* N^*, E^*, T^*, M^* *are corresponding optimal state variables of the control sys-*

The corresponding optimal control u^* is given as

$$u^*(t) = \min\left\{\max\left\{0, \frac{1}{\varepsilon_u B}(\lambda_3M^*T^* - \lambda_1M^*N^* - \lambda_2M^*E^* - \lambda_4W_M(t))\right\}, u_{\max}\right\}. \tag{34}$$

The proof will follow the work of Oke et al. [43].

Proof 12. Let u^* be the given optimal control function and N^*, E^*, T^*, M^* be the corresponding optimal states of the system that minimise the cost functional. We define the Hamiltonian denoted as $\mathscr{H}$ for the system (31) as follows:

$$\mathscr{H}(N, E, T, M, u, \lambda_1, \lambda_2, \lambda_3, \lambda_4) = L(N, E, T, M, u) + \lambda_1\frac{dN}{dt} + \lambda_2\frac{dE}{dt} + \lambda_3\frac{dT}{dt} + \lambda_4\frac{dM}{dt}.$$

Then, by the PMP, there exist adjoint variables λ_1, λ_2, λ_3 and λ_4 which satisfy the following equations:

$$\frac{d\lambda_1}{dt} = -\frac{\partial \mathscr{H}}{\partial N}, \quad \frac{d\lambda_2}{dt} = -\frac{\partial \mathscr{H}}{\partial E}, \quad \frac{d\lambda_3}{dt} = -\frac{\partial \mathscr{H}}{\partial T}, \quad \frac{d\lambda_4}{dt} = -\frac{\partial \mathscr{H}}{\partial M}, \tag{35}$$

with transversality conditions

$$\lambda_1(t_f) = \lambda_2(t_f) = \lambda_3(t_f) = \lambda_4(t_f) = 0.$$

Now,

$$\frac{d\lambda_1}{dt} = -\frac{\partial \mathscr{H}}{dN} = -\lambda_1(r_1 - 2r_1b_1N^* - c_1T^* - (1-u(t))M^*(t)) - \lambda_3c_2T^*,$$
$$\frac{d\lambda_2}{dt} = -\frac{\partial \mathscr{H}}{dE} = -\lambda_2\left(\frac{qT^*}{\alpha+T^*} - \mu - \beta T^* - (1-u(t))M^*(t)\right) + \lambda_3fT^*,$$
$$\frac{d\lambda_3}{dt} = -\frac{\partial \mathscr{H}}{dT} = -1 - \lambda_2\left(q\frac{E^*}{(\alpha+T^*)^2} - \beta E^*\right) + \lambda_1c_1N^* - \lambda_3(r_2 - 2r_2b_2T^* - fE^* - u(t)M^*(t) + c_2N^*),$$
$$\frac{d\lambda_4}{dt} = -\frac{\partial \mathscr{H}}{dM} = \lambda_1(1-u(t))N^* + \lambda_2(1-u(t))E^* + \lambda_3u(t)T^*, \tag{36}$$

evaluated at optimal control and corresponding states, resulting in the adjoint system (36). Therefore, from the optimality condition, we have

$$\frac{\partial \mathscr{H}}{\partial u} = 0 \text{ at } u = u^*, \tag{37}$$

and solving for u^* depending on the limits $0 < u_{\max} \leq 1$, the characterisation leads to the implication given in Equation (34):

$$\frac{\partial \mathscr{H}}{\partial u} = \varepsilon_u u^*(t)B + \lambda_1M^*(t)N^* + \lambda_2M^*(t)E^* - \lambda_3M^*(t)T^* + \lambda_4W_M(t) = 0.$$

4185, 2025, 1, Downloaded from https://onlinelibrary.wiley.com/doi/10.1155/jama/5536333 by South African Medical Research, Wiley Online Library on [24/11/2025]. See the Terms and Conditions (https://onlinelibrary.wiley.com/terms-and-conditions) on Wiley Online Library for rules of use; OA articles are governed by the applicable Creative Commons License

TABLE 1: Parameter values.

Parameter	Parameter description	Values	Units	Source
q	Degree of recruitment of maximum effector cells in relation with cancer cells	0.015	Day^{-1}	[20]
r_1	Rate of normal cell growth	0.4	Day^{-1}	Assumed, [47, 48]
r_2	Rate of tumour cell growth	0.005	Day^{-1}	Assumed
b_1	Capacity of normal cell	1.5	Cells^{-1}	Assumed, [46]
b_2	Capacity of tumour cell	0.975	Cells^{-1}	Assumed, [49]
f	Parameter of cancer cleanup	3.41×10^{-10}	Cell^{-1}	[20]
κ	Growth rate of normal/effector cells	1.25	Cells/day	Assumed, [20]
β	Degree of inactivation of effector cells	2×10^{-11}	Cells^{-1}	[20]
μ	Rate of natural demise of effector cells	2.5	Day^{-1}	Assumed
α	Curve of effector–immune cells	2.02×10^{5}	Day^{-1}	Assumed, [20]
ψ	Rate of decrease in concentration of chemotherapy drug	0.85	mg/m^2	Assumed, [20]
c_1	Competitive term	0.0004	Day^{-1}	Assumed, [18]
c_2	Competitive term	0.0002	Day^{-1}	Assumed
W_M	Amount of drug concentration	0.17, 0.25, varies	mg/m^2	Assumed
k_N	Control input that affects the normal cells	0.1	1/day	Assumed
k_E	Control input that affects the effector cells	0.1	1/day	Assumed
k_T	Control input that affects the tumour cells	0.5	1/day	Assumed
ε_u	Weighted factor	0.001	1/day	Assumed
B	Systematic cost	1.50	1/day	Assumed

TABLE 2: Summary of sensitivity analysis results.

Parameter	Mean	Std. dev.	S_i	S_{T_i}	Rank S_i	Rank S_{T_i}
μ	2.5	0.28881	0.90919	0.060673	2	4
b_1	1.5	0.28882	0.99109	0.00010504	6	5
f	$3.5e-10$	$2.888e-11$	0.95125	0.030827	5	1
r_2	0.0055	0.0025993	0.15381	0.81867	3	3
κ	1.25	0.1444	0.96251	0.065293	1	6
c_2	0.0002	$5.7761e-05$	0.99075	0.00021427	4	2

Hence, we obtain

$$u^*(t) = \frac{1}{\varepsilon_u B}(\lambda_3 M^*(t)T^* - \lambda_1 M^*(t)N^* - \lambda_2 M^*(t)E^* - \lambda_4 W_M(t)), \tag{38}$$

which is the singular function. Thus, by standard control arguments involving the bounds on controls, the optimal control takes the form

$$u^*(t) = \begin{cases} 0 & \text{if } \mathscr{H}_u < 0, \\ \frac{1}{\varepsilon_u B}(\lambda_3 M^*(t)T^* - \lambda_1 M^*(t)N^* - \lambda_2 M^*(t)E^* - \lambda_4 W_M(t)) & \text{if } \mathscr{H}_u = 0, \\ u_{\max} & \text{if } \mathscr{H}_u > 0. \end{cases} \tag{39}$$

□

5. Numerical Simulations

In this section, we present numerical results for the mathematical model with chemotherapy aiming to offer actionable and clinically relevant insights for adapting optimal control strategies in real-world cancer treatment scenarios. We used the Runge–Kutta method [44] to generate results for the model with no chemotherapy and for the application of chemotherapy using constant controls. We further used the forward–backward sweep method [45] to determine the optimal control results.

5.1. Parameter Estimation. In this section, the parameter values and initial values are estimated using data from the literature. In the numerical simulation, we use a similar technique that Itik et al. [46] used to avoid self-control of the immune system on the cancer cells by choosing a

4185, 2025, 1, Downloaded from https://onlinelibrary.wiley.com/doi/10.1155/jama/5536333 by South African Medical Research, Wiley Online Library on [24/11/2025]. See the Terms and Conditions (https://onlinelibrary.wiley.com/terms-and-conditions) on Wiley Online Library for rules of use; OA articles are governed by the applicable Creative Commons License

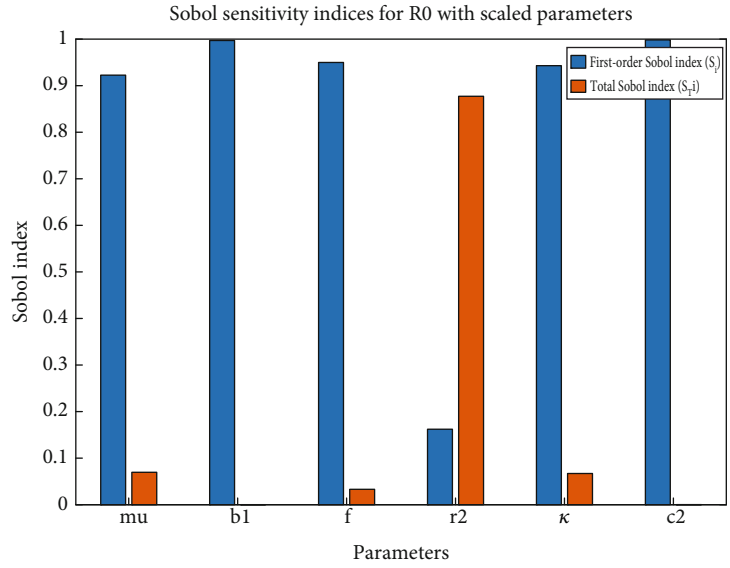

FIGURE 1: Sobol sensitivity indices for $\mathscr{R}_0$.

scenario where the initial immune cell population is very small and the tumour cell population is large, so that tumour growth is inevitable unless chemotherapy is applied. The initial conditions when the chemotherapy treatment is started are assumed to be $N(0) = 1.25$, $T(0) = 1.04$, $E(0) = 0.52$ and $M(0) = 0$.

Table 1 indicates the description of the parameters that are used and their values in the extended model of the tumour treatment with chemotherapy.

5.2. Sensitivity Analysis. To better understand the dynamic interactions within the tumour environment, sensitivity indices are computed. Sensitivity analysis is a quantitative approach that evaluates how model inputs, including parameters, affect model outputs [50]. The primary aim of sensitivity analysis is to identify which parameters significantly influence the output and which have minimal effect [51]. This process is essential for diagnosing the model structure and identifying key parameters, an important step in both model development and its subsequent application [52]. Sensitivity analysis can be categorised into two types: local and global sensitivity analysis (GSA). Local sensitivity analysis typically involves calculating partial derivatives using analytical or numerical methods, where one parameter is perturbed at a time [50]. However, this approach only examines the impact of individual parameters on the model output, without accounting for the interactions between multiple parameters. Furthermore, it cannot assess the combined influence of parameter interactions on the output [53]. According to Yang and Liu [53], whilst local sensitivity analysis is easy to implement, it has notable limitations due to the potential for the same effects to arise from different parameter combinations. To overcome these limitations, this study employs GSA, which evaluates the collective influence of multiple parameters and their interactions across the entire parameter space [53]. In contrast to local sensitivity analysis, GSA takes into account the distribution and shape

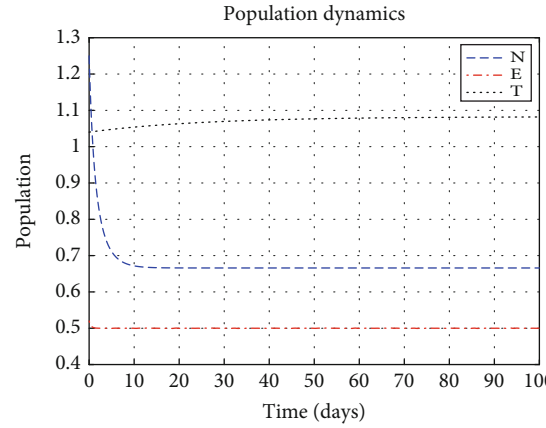

FIGURE 2: Cell populations without chemotherapy.

of the probability density functions of each parameter. Moreover, it allows for the simultaneous variation of all factors during the calculation and analysis, providing a more comprehensive understanding of parameter influences [53]. In this context, the goal is to identify the optimal threshold for chemotherapy drugs that will minimise pain for patients undergoing treatment. To achieve this, it is critical to understand the key factors influencing tumour growth. The initial growth of cancer is determined by the basic reproduction number $\mathscr{R}_0$, which drives the investigation into the sensitivity indices of this number in relation to specific model parameters. The following parameters are considered in the sensitivity analysis to assess their impact on the basic reproduction number: the capacity of normal cells (b_1), the rate of normal cell growth (r_1), the competitive effect of normal cells on tumour cell growth (c_2), the rate of tumour cell growth (r_2), the rate of natural demise of effector cells (μ), the cancer cleanup (f) and the growth rate of normal or effector cells (κ). GSA has proven effective in assessing the influence of uncertainties in various model components,

4185, 2025, 1, Downloaded from https://onlinelibrary.wiley.com/doi/10.1155/jama/5536333 by South African Medical Research, Wiley Online Library on [24/11/2025]. See the Terms and Conditions (https://onlinelibrary.wiley.com/terms-and-conditions) on Wiley Online Library for rules of use; OA articles are governed by the applicable Creative Commons License

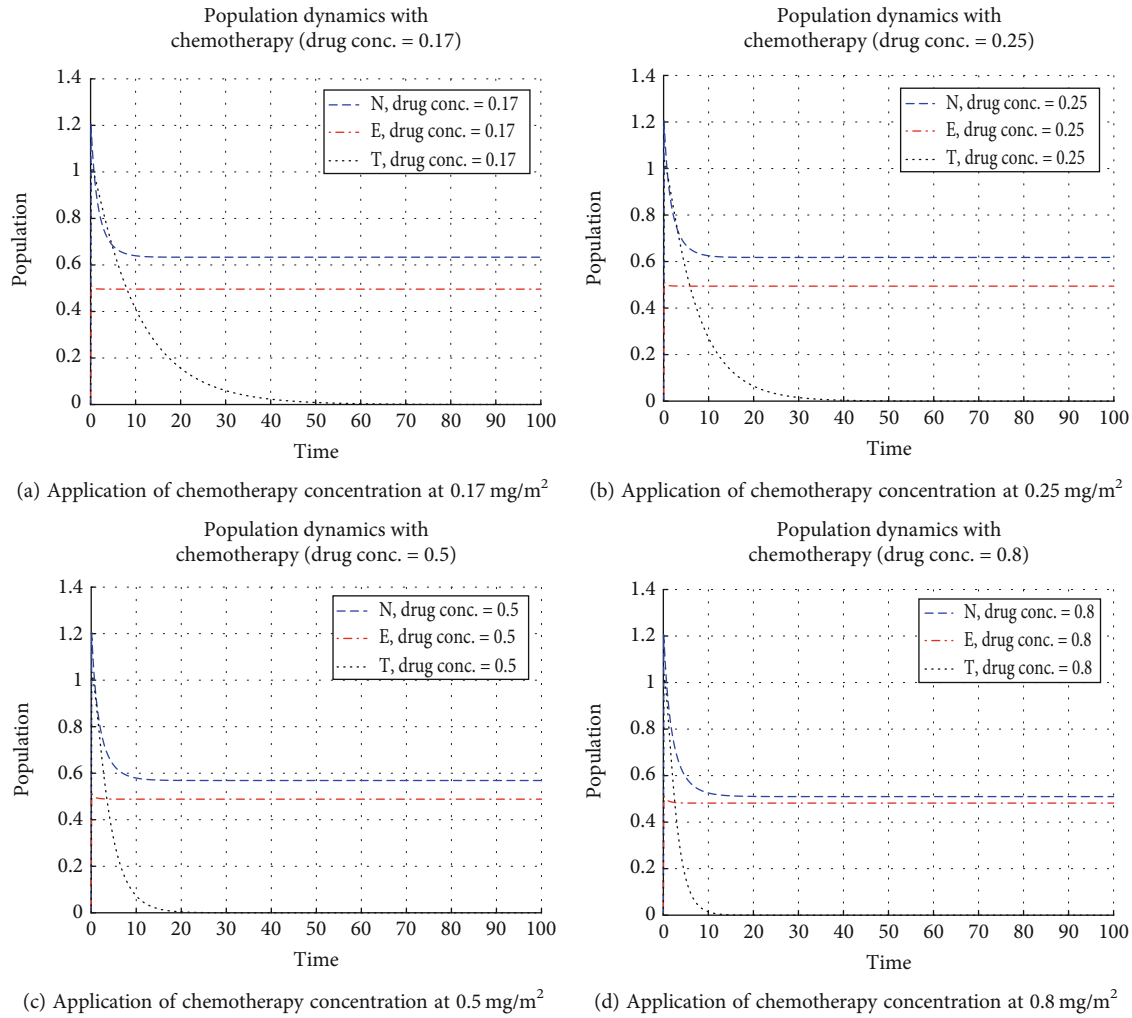
Population dynamics with chemotherapy (drug conc. = 0.17)
N, drug conc. = 0.17
E, drug conc. = 0.17
T, drug conc. = 0.17
Population
Time
Population dynamics with chemotherapy (drug conc. = 0.25)
N, drug conc. = 0.25
E, drug conc. = 0.25
T, drug conc. = 0.25
Population
Time
Population dynamics with chemotherapy (drug conc. = 0.5)
N, drug conc. = 0.5
E, drug conc. = 0.5
T, drug conc. = 0.5
Population
Time
Population dynamics with chemotherapy (drug conc. = 0.8)
N, drug conc. = 0.8
E, drug conc. = 0.8
T, drug conc. = 0.8
Population
Time

(a) Application of chemotherapy concentration at 0.17 mg/m^2

(b) Application of chemotherapy concentration at 0.25 mg/m^2

(c) Application of chemotherapy concentration at 0.5 mg/m^2

(d) Application of chemotherapy concentration at 0.8 mg/m^2

FIGURE 3: Application of chemotherapy concentrations.

such as parameters, initial conditions and boundary conditions, on model behaviour and predictions [54]. Consequently, the GSA method, initially introduced by Saltelli et al. [50] and further developed by Yang and Liu [53], is applied in this study. The methodology is implemented using a MATLAB script, which computes global sensitivity indices based on the Sobol method. This approach is used to analyse the impact of parameters on the basic reproduction number $\mathscr{R}_0$ in the model. The process begins by defining the parameter ranges (LB and UB) and 95% confidence intervals (CIs) for each parameter, such as $\mu \in [2.0, 3.0]$ with a CI of $[2.3, 2.7]$, which guides the sampling process. Sample matrices A and B are then generated using Latin hypercube sampling (LHS), ensuring uniform coverage of the parameter space. These samples are subsequently scaled to the defined parameter ranges using the following formula:

$$\text{Value} = \text{LB} + (\text{UB} - \text{LB}) \times \text{normalised sample}.$$

This scaling ensures that the sampled values fall within the biologically plausible ranges specified for each parameter. The script proceeds to evaluate the formula for $\mathscr{R}_0$, for each row in matrices A and B, resulting in vectors $\mathscr{R}_{0A}$ and $\mathscr{R}_{0B}$. The total variance of $\mathscr{R}_0$ is calculated as

$$\text{Total\_var} = \text{var}\left([\mathscr{R}_{0A}\,;\mathscr{R}_{0B}]\right).$$

For each parameter, the first-order Sobol indices (S_i) and total Sobol indices (S_{T_i}) are computed using the following formulas:

$$S_i = \frac{\text{mean}\left(\mathscr{R}_{0A} \cdot \mathscr{R}_{0C_i}\right) - \text{mean}\left(\mathscr{R}_{0A}\right)^2}{\text{total\_var}},$$

$$S_{T_i} = \frac{0.5 \cdot \text{mean}\left(\left(\mathscr{R}_{0A} - \mathscr{R}_{0C_i}\right)^2\right)}{\text{total\_var}},$$

where $\mathscr{R}_{0C_i}$ is the $\mathscr{R}_0$ values computed using the hybrid matrix C_i. Finally, the results, including the mean, standard deviation, Sobol indices and parameter rankings, are displayed in a table providing a comprehensive analysis of parameter influence on $\mathscr{R}_0$. This approach aligns with the

4185, 2025, 1, Downloaded from https://onlinelibrary.wiley.com/doi/10.1155/jama/5536333 by South African Medical Research, Wiley Online Library on [24/11/2025]. See the Terms and Conditions (https://onlinelibrary.wiley.com/terms-and-conditions) on Wiley Online Library for rules of use; OA articles are governed by the applicable Creative Commons License

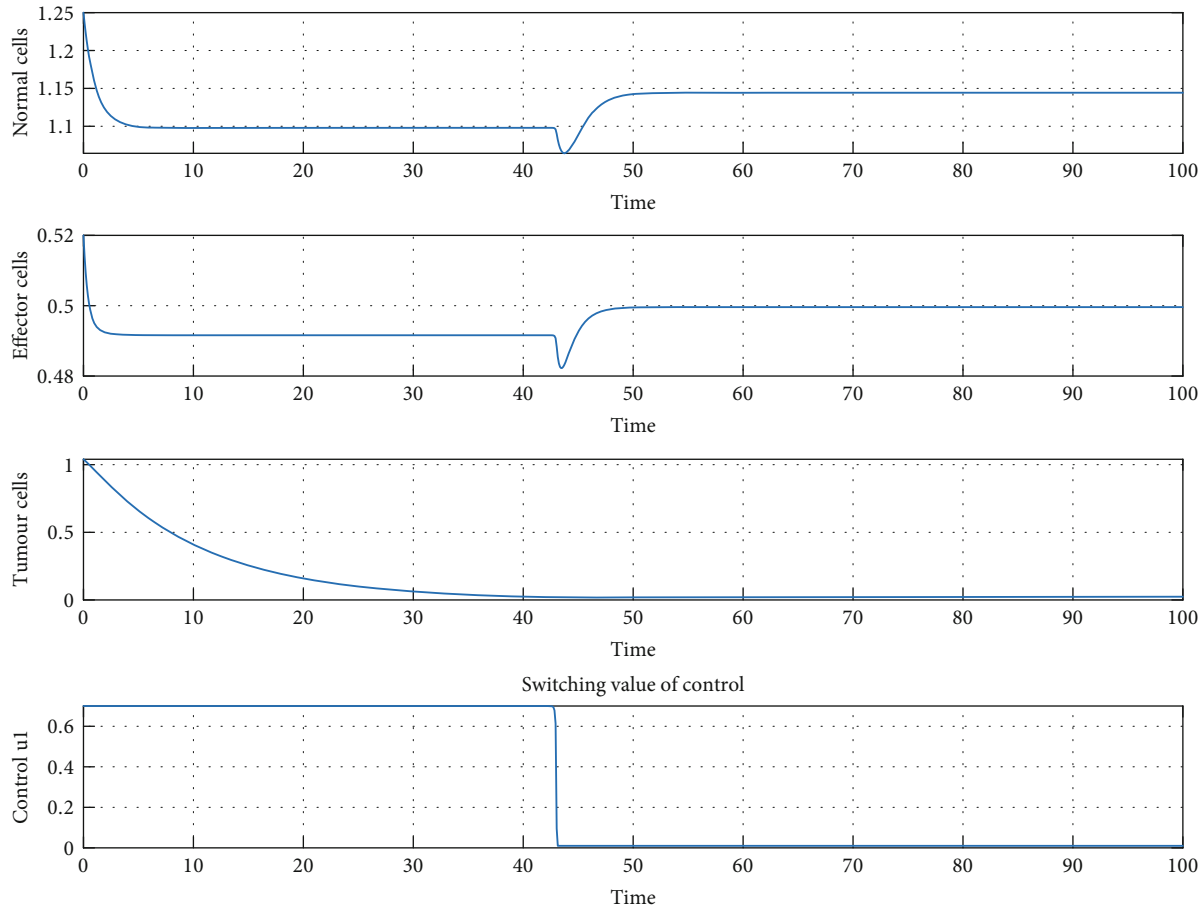

Figure 4: Optimal states with chemotherapy drug at 0.17 mg/m^2.

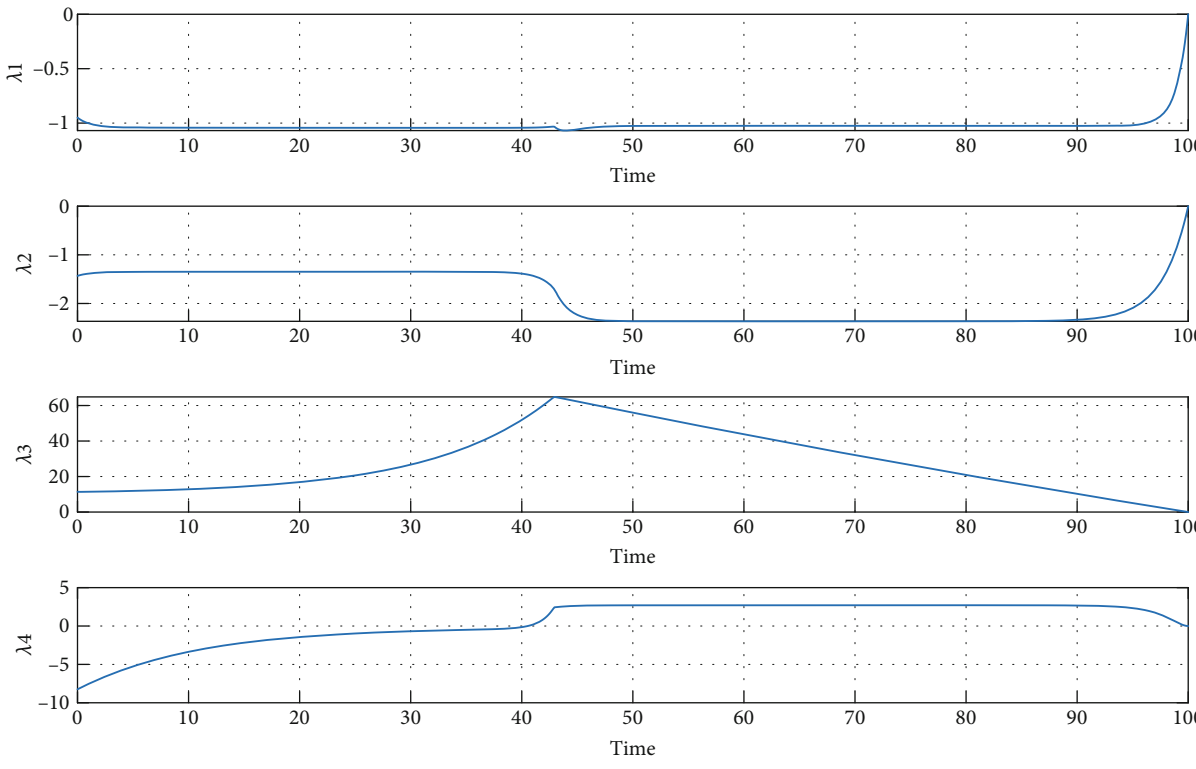

Figure 5: Adjoint of the system at the drug concentration of 0.17 mg/m^2.

4185, 2025, 1, Downloaded from https://onlinelibrary.wiley.com/doi/10.1155/jama/5536333 by South African Medical Research, Wiley Online Library on [24/11/2025]. See the Terms and Conditions (https://onlinelibrary.wiley.com/terms-and-conditions) on Wiley Online Library for rules of use; OA articles are governed by the applicable Creative Commons License

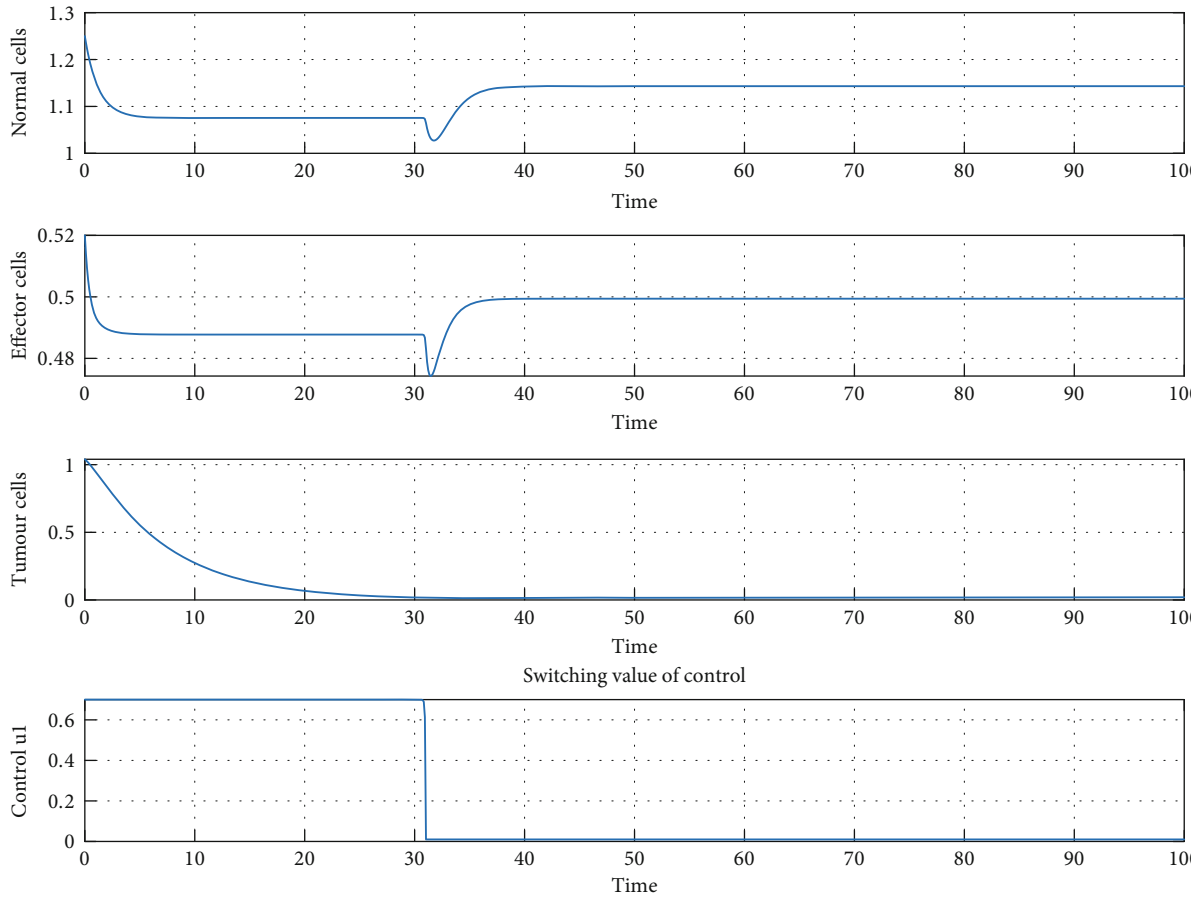

FIGURE 6: Optimal states with chemotherapy drug at 0.25 mg/m^2.

methodology described by Yang and Liu [53] and ensures robust sensitivity analysis for the disease-information coupling model. The results, displayed in Table 2, show the summary of the parameters by their influence, aligning with the methodology described in [53] for identifying key drivers of disease dynamics.

The sensitivity analysis results reveal that the most influential parameters, based on total-order indices (S_{T_i}), are f, c_2 and r_2. The parameter f has the highest total-order index ($S_{T_i} = 0.030827$, Rank 1), indicating significant influence primarily through interactions with other parameters. Similarly, c_2 ($S_{T_i} = 0.00021427$, Rank 2) and r_2 ($S_{T_i} = 0.81867$, Rank 3) also exhibit substantial total effects, with r_2 showing particularly strong interactions due to its low first-order index ($S_i = 0.15381$) relative to its total-order index. In contrast, κ and μ have high first-order indices ($S_i = 0.96251$ and 0.90919, respectively), indicating strong independent effects, but their total-order indices are relatively low, suggesting limited interactions. The parameter b_1 is the least influential, with both low first-order and total-order indices. Overall, f, c_2 and r_2 are the key drivers of output variance, with f being the most critical due to its dominant total-order effect. These findings are visually summarised in Figure 1, which illustrates the relative importance of each parameter. The results align well with the dynamics of disease spread and control strategies, providing valuable insights into the model's behaviour.

5.3. Results. In this section, the optimal control and corresponding states associated with the optimal strategy are shown graphically.

Figure 2 illustrates a mathematical model portraying cell population without chemotherapy or drugs, detailed in system (1). The visualisation depicts how tumours affect the cell population in the human system before chemotherapy is introduced, emphasising the issue of tumour growth leading to a reduction in healthy cell numbers. The graph reveals a clear trend; an increase in tumour cell count corresponds to a decrease in both normal and effector cell populations. The decline in normal cells is due to their transformation into tumour cells, influenced by aggressive tumour growth. Immune cells also diminish as they are affected by tumour growth, with tumours competing for resources with healthy cells.

5.3.1. Model With Constant Chemotherapy Application. In this subsection, we discuss the results for the model with chemotherapy at constant preset values of $k_N = 0.1$, $k_E = 0.1$ and $k_T = 0.5$. Figure 3a presents what happens at a drug concentration of 0.17 mg/m^2. The system exhibits a moderate response. The normal cell population undergoes a gradual decline, reaching a stable level of 0.604 by the 10th day. This behaviour suggests that the chemotherapy at this concentration effectively controls normal cell growth without

4185, 2025, 1, Downloaded from https://onlinelibrary.wiley.com/doi/10.1155/jama/5536333 by South African Medical Research, Wiley Online Library on [24/11/2025]. See the Terms and Conditions (https://onlinelibrary.wiley.com/terms-and-conditions) on Wiley Online Library for rules of use; OA articles are governed by the applicable Creative Commons License

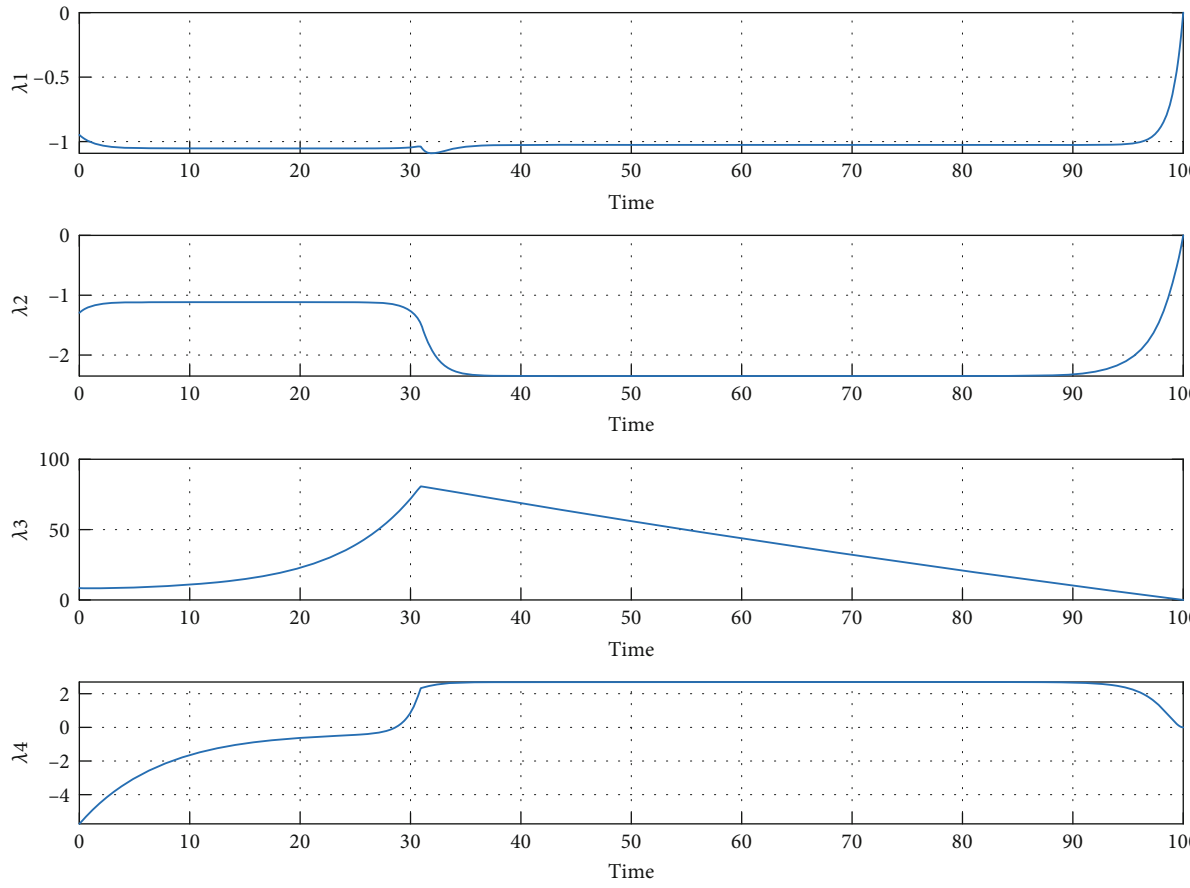

FIGURE 7: Adjoint of the system at the drug concentration of 0.25 mg/m^2.

causing an abrupt decline. The sustained suppression of effector cells at 0.496 indicates a prolonged impact on the immune response, possibly compromising the body's ability to mount an effective defence against cancer cells. The tumour cell population shows a slow response, reaching elimination on the 50th day, reflecting the lower potency of the treatment. The delayed elimination could be attributed to the relatively lower drug concentration, requiring an extended treatment period for efficacy.

Figure 3b presents what happens at a drug concentration of 0.25 mg/m^2 as the system demonstrates a more efficient response. The normal cell population undergoes a gradual decline, stabilising at 0.6470 by the 10th day. This indicates that the chemotherapy is effective in controlling normal cell growth whilst achieving a balance that allows for some recovery. Effector cells are sustained at 0.494, showcasing a persistent impact on the immune response, albeit at a slightly lower level than the lower drug concentration. The tumour cells exhibit a more rapid response, reaching elimination on the 39th day. This suggests an increased potency of the treatment, allowing for a more efficient control of tumour growth whilst still maintaining a balance with normal cell populations.

Figure 3c presents the system dynamics shift upon increasing the drug concentration to 0.5 mg/m^2. Normal cell populations gradually decline, stabilise at 0.587 after the tumour is eradicated on the 30th day and display a slight recovery. This indicates a balanced response, efficiently controlling tumour cells whilst allowing for a controlled recovery of normal cells. Effector cells remain suppressed at 0.489, maintaining a balance between immune system suppression and tumour control. The gradual decrease in tumour cells and elimination on the 20th day further support the idea of a well-balanced response, effectively targeting the tumour without causing undue damage to normal cells.

At the highest drug concentration of 0.8 mg/m^2, shown in Figure 3d, the system exhibits a swift and potent response. Normal cells experience a rapid decline, stabilising at 0.528. This abrupt nature of the decline suggests a highly effective yet aggressive impact on normal cells. Effector cells also show rapid and sustained suppression, stabilising at 0.481 on the 20th day, indicating a potent and persistent impact on the immune response. The tumour cells respond swiftly, reaching elimination on the 12th day, showcasing the high potency of the treatment. However, the abrupt impact on normal and effector cells raises concerns about potential side effects and challenges to overall immune function.

Increasing the drug dosage leads to a faster elimination of tumour cells, but it also causes a more rapid decline in normal and effector cell populations. At lower concentrations, such as 0.17 mg/m^2, the system shows a more gradual and controlled response, with tumour cells eliminated after 50 days and minimal impact on normal cells. As the dosage

4185, 2025, 1, Downloaded from https://onlinelibrary.wiley.com/doi/10.1155/jama/5536333 by South African Medical Research, Wiley Online Library on [24/11/2025]. See the Terms and Conditions (https://onlinelibrary.wiley.com/terms-and-conditions) on Wiley Online Library for rules of use; OA articles are governed by the applicable Creative Commons License

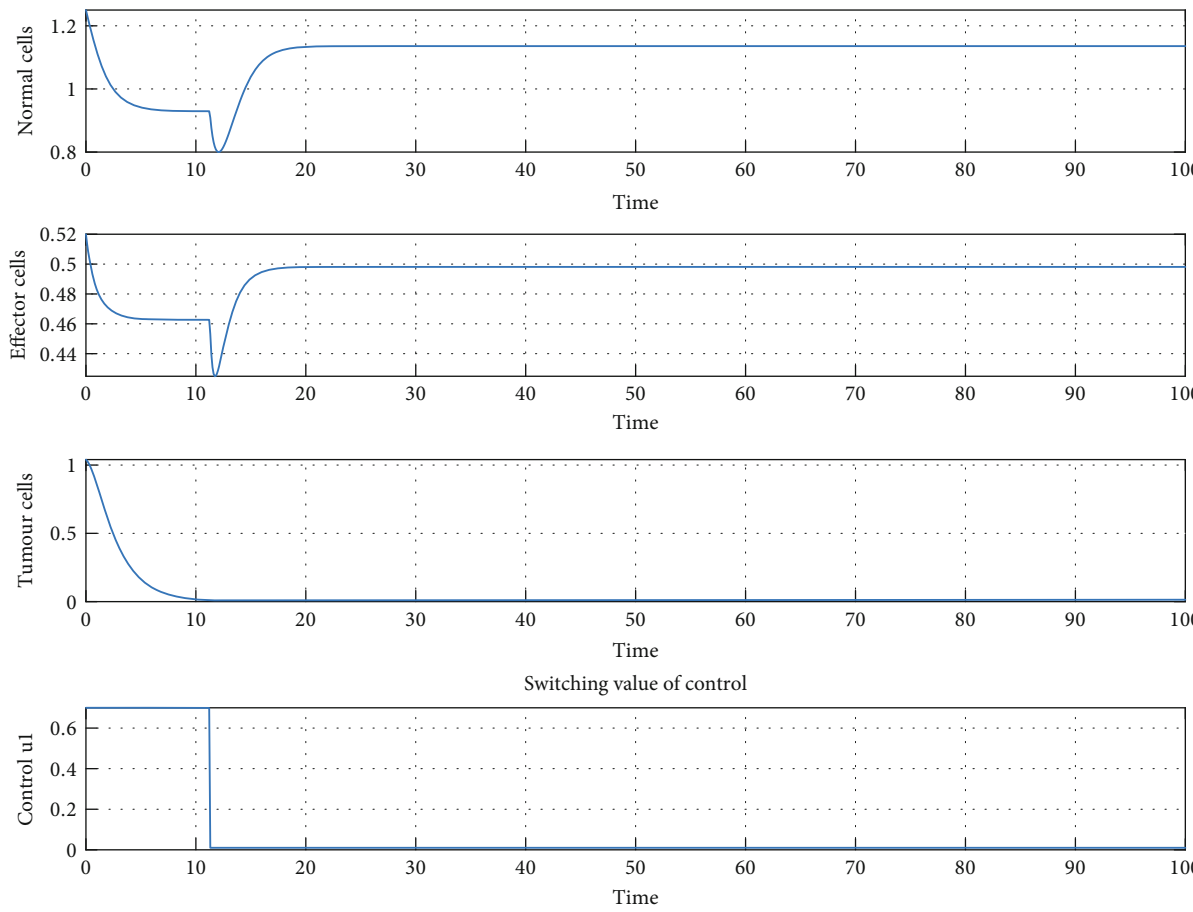

Figure 8: Optimal states with chemotherapy drug of 0.8 mg/m^2.

increases, the tumour eradication becomes quicker, with tumour cells eliminated within 12 days at 0.8 mg/m^2. However, this higher potency comes with a more aggressive impact on normal and effector cells, indicating stronger side effects and potential immune suppression. The positive aspect of increasing dosage is the faster tumour control, which could be crucial in aggressive cancer cases, but the negative side involves greater harm to healthy cells and immune function, leading to potential complications.

5.3.2. Optimal Control Results. The results of the mathematical model describing tumour treatment with chemotherapy reveal dynamic interactions between the administered drug, cell populations and adjoint variables (lambdas) over a 100-day period.

Figure 4 illustrates the effect of a 0.17 mg/m^2 chemotherapy concentration. The normal cell population initially drops from 1.25 to 1.13 within the first 5 days, continuing to decrease to 1.01 by Day 43. Afterward, it rebounds to 1.14 by Day 50, maintaining this level even after tumour cells are eradicated on Day 41. The effector cells also show an initial decline and stabilise around 0.50 after the tumour is eliminated. Tumour cells decrease significantly from 1.04 to 0.665 within 5 days and are fully eradicated by Day 41. The control u remains at its maximum value, $u_{max} = 0.7$, from time $t = 0$ until $t = 43.1$ days, applying constant treatment to suppress the tumour. At $t = 43.3$ days, the control switches from $u_{max} = 0.7$ to its minimum value, $u_{min} = 0$, as the tumour has been eliminated. After this point, the control stays at $u_{min} = 0$, as no further treatment is required once the tumour has been cleared. In Figure 5, the adjoint variables for a 0.17 mg/m^2 chemotherapy concentration exhibit notable variations. The adjoint variable λ_1 for normal cells decreases over time, reflecting the negative impact of increases in normal cell populations on the system. The adjoint variable λ_2 for effector cells initially increases and then decreases significantly, indicating heightened sensitivity to changes in effector cell populations. The adjoint variable λ_3 for tumour cells shows a sharp rise followed by a decline, which mirrors the dynamics of tumour control and underscores the critical treatment period.

Figure 6 depicts the effect of a 0.25 mg/m^2 chemotherapy concentration. The normal cell population initially declines from 1.25 to 1.10 by Day 5, stabilises until Day 30, then drops to 1.05 on Day 32 before rising to 1.14 by Day 40. Effector cells decline from 0.52 to 0.488, with a critical drop to 0.475 on Day 32 and recovery to 0.50 by Day 40. Tumour cells decrease from 1 to 0.554 by Day 5 and are eradicated by Day 30. The control u remains at its maximum value, $u_{max} = 0.7$, from time $t = 0$ until $t = 31.03$ days, applying constant treatment to suppress the tumour. At $t = 46.1$ days, the

4185, 2025, 1, Downloaded from https://onlinelibrary.wiley.com/doi/10.1155/jama/5536333 by South African Medical Research, Wiley Online Library on [24/11/2025]. See the Terms and Conditions (https://onlinelibrary.wiley.com/terms-and-conditions) on Wiley Online Library for rules of use; OA articles are governed by the applicable Creative Commons License

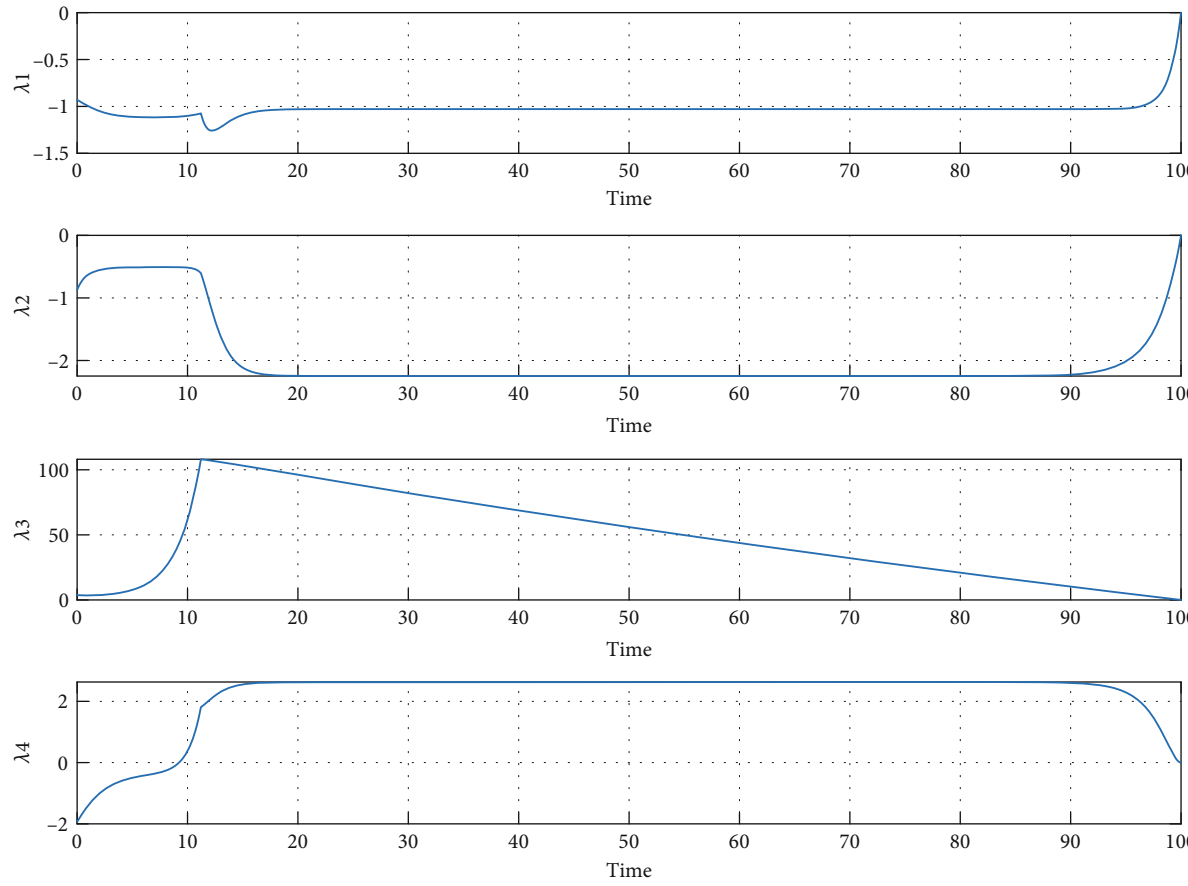

FIGURE 9: Adjoint of the system at the drug concentration of 0.8 mg/m^2.

control switches from $u_{max} = 0.7$ to its minimum value, $u_{min} = 0$, as the tumour has been eliminated. After this point, the control stays at $u_{min} = 0$, as no further treatment is required once the tumour has been cleared. Figure 7 shows the adjoint variables for a 0.25 mg/m^2 chemotherapy concentration. The adjoint variable λ_1 for normal cells decreases over time, reflecting how changes in normal cell dynamics impact the system. The adjoint variable λ_2 for effector cells shows an initial increase followed by a significant drop, indicating variations in sensitivity to effector cell dynamics. The adjoint variable λ_3 rises sharply and then declines, mirroring tumour dynamics and highlighting the sensitivity of tumour control. The adjoint variable λ_4 starts negative, increases and then decreases, reflecting the impact of drug concentration on the system.

Figure 8 depicts the effect of a 0.8 mg/m^2 chemotherapy concentration. The normal cell population drops from 1.25 to 0.96 on Day 5, continues to decrease to 0.82 on Day 12 and then recovers to 1.16 by Day 30. Effector cells decline from 0.52 to 0.465 by Day 11, recovering to 0.498 by Day 30. Tumour cells decrease from 1 to 0.171 by Day 5 and are eradicated by Day 10. The control u remains at its maximum value, $u_{max} = 0.7$, from time $t = 0$ until $t = 11.2$ days, applying constant treatment to suppress the tumour. At $t = 11.4$ days, the control switches from $u_{max} = 0.7$ to its minimum value, $u_{min} = 0$, as the tumour has been eliminated. After this point, the control stays at $u_{min} = 0$, as no further treatment is required once the tumour has been cleared. Figure 9 shows the adjoint variables for a 0.8 mg/m^2 chemotherapy concentration. The adjoint variable λ_1 for normal cells decreases over time, with a notable drop on Day 12, reflecting the impact of changes in normal cell populations on the system. The adjoint variable λ_2 for effector cells initially rises and then significantly decreases, indicating variations in sensitivity to changes in effector cell populations. The adjoint variable λ_3 shows a sharp rise and subsequent decline, mirroring the dynamics of tumour cell control. The adjoint variable λ_4 increases, reflecting how the drug concentration affects the system.

Furthermore, the switching times decrease with increasing dosage or drug concentration. The most notable finding is that normal and immune cells recover when the tumour is cleared. However, they do not recover to original levels indicating the adverse or unintended effect chemotherapy has on normal and immune cells. There is a slight delay in recovery which can be attributed to the excess drug that may still be in the body when the tumour is cleared.

6. Discussion and Conclusion

The study provides a comprehensive analysis of the normal-tumour interaction under chemotherapy intervention, utilising mathematical modelling and numerical simulations validated through MATLAB. The mathematical analysis

4185, 2025, 1, Downloaded from https://onlinelibrary.wiley.com/doi/10.1155/jama/5536333 by South African Medical Research, Wiley Online Library on [24/11/2025]. See the Terms and Conditions (https://onlinelibrary.wiley.com/terms-and-conditions) on Wiley Online Library for rules of use; OA articles are governed by the applicable Creative Commons License

highlights that the basic reproduction number ($\mathscr{R}_0$) is a critical determinant of tumour dynamics. Values of $\mathscr{R}_0$ below 1 suggest a stable tumour-free equilibrium, indicating effective control of tumour spread. Conversely, values exceeding 1 imply potential metastasis, emphasising the need for vigilant monitoring and intervention. In the study, the Lyapunov function serves as a vital tool for analysing the stability of the tumour dynamics. By constructing a Lyapunov function tailored to the system's dynamics, the authors demonstrate that the tumour-free equilibrium is globally asymptotically stable when the basic reproduction number ($\mathscr{R}_0$) is less than 1. This stability indicates that, with appropriate treatment strategies, the tumour can be effectively controlled and eliminated. The Lyapunov function not only confirms the theoretical predictions of the model but also provides a framework for understanding how perturbations in tumour behaviour can be managed. OCP was considered after Lyapunov function analysis. The study thus highlights the importance of mathematical modelling in deriving insights into tumour dynamics and informing treatment protocols. The equilibrium points, tumour-free, Type 1 dead, Type 2 dead and endemic, offer insights into the long-term behaviour of the system, guiding the development of treatment strategies. The analysis also demonstrates that optimal control strategies can effectively promote the recovery of normal and effector cells after treatment whilst ensuring timely cessation of therapy once the tumour is eradicated. Balancing treatment intensity with patient safety is crucial for optimising therapeutic outcomes.

GSA was conducted to understand the dynamic interactions within the tumour environment and identify key parameters influencing tumour dynamics and treatment outcomes. The results reveal that the most influential parameters affecting the basic reproduction number $\mathscr{R}_0$ are the cancer cleanup f, the competitive effect of normal cells on tumour cell growth c_2 and the rate of tumour cell growth r_2. The dominance of f in total-order sensitivity indices highlights its critical role in tumour progression and treatment response. Whilst r_2 exhibited strong interaction effects, parameters κ and μ showed high independent effects but minimal interactions. The least influential parameter was b_1, contributing negligibly to $\mathscr{R}_0$. These findings emphasise the importance of accurate parameter estimation and the need to account for parameter interactions in optimising chemotherapy strategies. By leveraging GSA, this study provides crucial insights for improving predictive models and developing more effective therapeutic interventions in oncology.

Numerical simulations reveal distinct patterns based on varying chemotherapy drug concentrations. Figure 2 illustrates how tumour growth leads to a decrease in both normal and effector cells, consistent with findings from Rokforoz et al. [55] and Ghaffari and Nasserifar [56], who similarly noted the detrimental impact of tumour proliferation on healthy cells. At lower concentration, the normal cell population gradually declines, whilst the tumour cells are eliminated slowly. Increasing the drug concentration results in faster clearing of tumour cells, but this comes at the cost of a rapid decline in normal cells and immune cell populations, reflecting potential side effects and immune suppression. The study confirms that $\mathscr{R}_0$ is a crucial determinant of tumour dynamics, with values less than 1 indicating a stable tumour-free equilibrium and values greater than 1 suggesting potential metastasis. Optimal control strategies were shown to be effective in promoting recovery of normal and effector cells posttreatment and ensuring timely cessation of therapy once the tumour is eradicated. Treatment approaches demonstrated include constant chemotherapy application (Figure 4), which achieves tumour clearance but lacks guidance on treatment cessation, and optimal control (Figures 6, 7 and 8), which identifies optimal times to switch treatment levels and minimises adverse drug effects. This is in agreement with the work and findings of Borah et.al [57], who studied the dynamics of COVID-19 propagation with vaccination and optimal control strategies. Their results indicated that implementing time-dependent interventions dynamically adjusts intervention levels based on the current epidemic state, leading to reduced disease transmission and overall infection burden.

In conclusion, this study highlights the necessity for personalised chemotherapy regimens that consider both treatment efficacy and potential side effects. The integration of optimal control strategies into chemotherapy planning can significantly improve patient outcomes by minimising harm whilst effectively targeting tumour cells. The findings indicate that whilst higher drug concentrations accelerate tumour elimination, they also pose risks of increased toxicity and immune suppression. Sensitivity analysis confirms the critical importance of accurate parameter estimation for optimising treatment protocols. Future research should focus on validating these results through experimental studies to ensure the model's practical applicability and further advance individualised cancer treatment strategies. Addressing these areas will enhance the understanding and management of chemotherapy in cancer treatment.

Data Availability Statement

The data used to support the findings of this study was obtained and also estimated from literature.

Conflicts of Interest

The authors declare no conflicts of interest.

Funding

No funding was received for this manuscript.

References

[1] C. A. Almeida and S. A. Barry, *Cancer Basic Science and Clinical Aspects* (A John Wiley & Sons, Ltd, Publication, 2010).

[2] International Agency for Research on Cancer, "Latest Global Cancer Data: Cancer Burden Rises to 19.3 Million New Cases and 10.0 Million Cancer Death in 2020" Accessed April 3, 2022, https://www.iarc.who.int/wp-content/uploads/2020/12/pr292_E.pdf.

4185, 2025, 1, Downloaded from https://onlinelibrary.wiley.com/doi/10.1155/jama/5536333 by South African Medical Research, Wiley Online Library on [24/11/2025]. See the Terms and Conditions (https://onlinelibrary.wiley.com/terms-and-conditions) on Wiley Online Library for rules of use; OA articles are governed by the applicable Creative Commons License

[3] A. Jemal, F. Bray, M. M. Center, J. Ferlay, E. Ward, and D. Forman, "Global Cancer Statistics," *CA: A Cancer Journal for Clinicians* 61, no. 2 (2011): 69–90, https://doi.org/10.3322/caac.20107.

[4] D. M. Parkin, F. Bray, J. Ferlay, and A. Jemal, "Cancer in Africa 2012," *Cancer Epidemiology, Biomarkers & Prevention* 23 (2014): 953–966, https://doi.org/10.1158/1055-9965.EPI-14-0281.

[5] T. R. Rebbeck, "Cancer in Sub-Saharan Africa," *Science* 367, no. 6473 (2020): 27–28, https://doi.org/10.1126/science.aay4743.

[6] C. D. Mathers and D. Loncar, "Projections of Global Mortality and Burden of Disease From 2002 to 2030," *PLoS Medicine* 3, no. 11 (2006): e442, https://doi.org/10.1371/journal.pmed.0030442.

[7] World Health Organization, "World Health Organization, International Agency for Research on Cancer. 1 February 2024" accessed April 22, 2025, https://www.who.int/news/item/01-02-2024-global-cancer-burden-growing%2D%2Damidst-mounting-need-for-services.

[8] "National Cancer Strategic Framework 2017-2022, South Africa," Accessed April 4, 2022 https://www.health.gov.za/wp-content/uploads/2020/11/national-cancer-strategic-framework-2017-2022-min.pdf.

[9] International Agency for Research on Cancer, "South Africa, 2020" Accessed June 3, 2022, https://cansa.org.za/files/2021/02/IARC-Globocan-SA-2020-Fact-Sheet.pdf.

[10] K. C. Calman, J. F. Smyth, and M. H. N. Tattersall, *Basic Principles of Cancer Chemotherapy* (The Macmillan Press LTD., 1980).

[11] L. Minasiah, O. Rosen, D. Auclair, A. Rahman, R. Pazdur, and R. Schilsky, "Optimizing Dosing of Oncology Drugs," *Clinical Pharmacology & Theorapeutics* 96, no. 5 (2014): 572–579, https://doi.org/10.1038/clpt.2014.153.

[12] D. Crosby, S. Bhatia, K. M. Brindle, et al., "Early Detection of Cancer," *Science* 375, no. 6586 (2022): eaay9040, https://doi.org/10.1126/science.aay9040.

[13] J. D. Schiffman, P. G. Fisher, and P. Gibbs, "Early Detection of Cancer: Past, Present, and Future," *American Society of Clinical Oncology Educational Book* 35, no. 1 (2015): 57–65, https://doi.org/10.14694/EdBook_AM.2015.35.57.

[14] I. Jena, K. Dehingia, A. Kullu, and A. Priyadarshi, "Bifurcation Analysis of a Discrete-Time Tumor Model With Crowley-Martin Functional Response and Its Optimal Control Theory," *Iranian Journal of Science* 49, no. 4 (2025): 1125–1144, https://doi.org/10.1007/s40995-025-01796-z.

[15] M. A. Alqudah, "Cancer Treatment by Stem Cells and Chemotherapy as a Mathematical Model With Numerical Simulations," *Alexandria Engineering Journal* 59, no. 4 (2020): 1953–1957, https://doi.org/10.1016/j.aej.2019.12.025.

[16] G. Song, G. Liang, T. Tian, and X. Zhang, "Mathematical Modeling and Analysis of Tumor Chemotherapy," *Symmetry* 14, no. 4 (2022): 704, https://doi.org/10.3390/sym14040704.

[17] S. T. R. Pinho, H. I. Freedman, and F. Nani, "A Chemotherapy Model for the Treatment of Cancer With Metastasis," *Journal of Mathematical and Computer Modelling* 36, no. 7-8 (2002): 773–803, https://doi.org/10.1016/S0895-7177(02)00227-3.

[18] L. G. De Pillis and A. Radunskaya, "The Dynamics of an Optimally controlled tumor Model: A case study," *Mathematical and Computer Modelling* 37, no. 11 (2003): 1221–1244, https://doi.org/10.1016/S0895-7177(03)00133-X.

[19] N. H. Sweilam, S. M. Al-Mekhlafi, T. Assiri, and A. Atangana, "Optimal Control for Cancer Treatment Mathematical Model Using Atangana-Baleanu-Caputo Fractional Derivative," *Advances in Difference Equations* 2020 (2020): 334, https://doi.org/10.1186/s13662-020-02793-9.

[20] D. Lestari, E. R. Sari, and H. Arifah, "Dynamics of a Mathematical Model of Cancer Cells With Chemotherapy," *Journal of Physics: Conference Series* 1320 (2019): 1–9, https://doi.org/10.1088/1742-6596/1320/1/012026.

[21] K. Dehingia, S. A. Alharbi, A. Jahman Alqarni, et al., "Exploring the Combined Effect of Optimally Controlled Chemo-Stem Cell Therapy on a Fractional-Order Cancer Model," *PLoS One* 20, no. 2 (2025): e0311822, https://doi.org/10.1371/journal.pone.0311822.

[22] R. I. Salih, S. Jawad, K. Dehingia, and A. Das, "The Effect of a Psychological Scare on the Dynamics of the Tumor-Immune Interaction With Optimal Control Strategy," *An International Journal of Optimization and Control: Theories & Applications (IJOCTA)* 14, no. 3 (2024): 276–293, https://doi.org/10.11121/ijocta.1520.

[23] L. G. De Pillis and A. Radunskaya, "A Mathematical Tumor Model With Immune Resistance and Drug Therapy: An Optimal Control Approach," *Computational and Mathematical Methods in Medicine* 3, no. 2 (2001): 79–100, https://doi.org/10.1080/10273660108833067.

[24] L. A. Emens and G. Middleton, "The Interplay of Immunotherapy and Chemotherapy: Harnessing Potential Synergies," *Cancer Immunology Research* 3, no. 5 (2015): 436–443, https://doi.org/10.1158/2326-6066.CIR-15-0064.

[25] R. Eftimie, J. L. Bramson, and D. J. Earn, "Interactions Between the Immune System and Cancer: A Brief Review of Non-Spatial Mathematical Models," *Bulletin of Mathematical Biology* 73, no. 1 (2011): 2–32, https://doi.org/10.1007/s11538-010-9526-3.

[26] X. Lai and A. Friedman, "Combination Therapy of Cancer With Cancer Vaccine and Immune Checkpoint Inhibitors: A Mathematical Model," *PLoS One* 12, no. 5 (2017): e0178479, https://doi.org/10.1371/journal.pone.0178479.

[27] P. Liu and X. Liu, "Dynamics of a Tumor-Immune Model Considering Targeted Chemotherapy," *Chaos, Solution & Fractals* 98 (2017): 7–13, https://doi.org/10.1016/j.chaos.2017.03.002.

[28] E. D. Gurmu and P. R. Koya, "Impact of Chemotherapy Treatment on SITR Compartmentalization and Modeling of Human Papilloma Virus (HPV)," *IOSR Journal of Mathematics (IOSR-JM)* 15, no. 3 (2019): 17–29, https://doi.org/10.9790/5728-1503011729.

[29] S. O. Sowole, D. Sangare, A. A. Ibrahim, and I. A. Paul, "On the Existence, Uniqueness, Stability of Solution and Numerical Simulations of a Mathematical Model for Measles Disease," *International Journal of Advances in Mathematics* 4, no. 2019 (2019): 84–111.

[30] E. A. Coddington and N. Levinson, *Theory of Ordinary Differential Equations* (McGraw-Hill, 1955).

[31] J. Á. Cid, "On Uniqueness Criteria for Systems of Ordinary Differential Equations," *Journal of Mathematical Analysis and Applications* 281, no. 1 (2003): 264–275, https://doi.org/10.1016/S0022-247X(03)00073-6.

[32] G. Teschl, *Ordinary Differential Equations and Dynamical Systems* 140, American Mathematical Society, 2024).

[33] E. A. Coddington, *An Introduction to Ordinary Differential Equations* (Courier Corporation, 2012).

[34] A. C. Peterson, "Existence-Uniqueness for Ordinary Differential Equations," *Journal of Mathematical Analysis and*

4185, 2025, 1, Downloaded from https://onlinelibrary.wiley.com/doi/10.1155/jama/5536333 by South African Medical Research, Wiley Online Library on [24/11/2025]. See the Terms and Conditions (https://onlinelibrary.wiley.com/terms-and-conditions) on Wiley Online Library for rules of use; OA articles are governed by the applicable Creative Commons License

Applications 64, no. 1 (1978): 166–172, https://doi.org/10.1016/0022-247X(78)90029-X.

[35] G. F. Simmons, *Differential Equations With Applications and Historical Notes* (CRC Press, 2016).

[36] A. Padder, S. Qureshi, R. S. Dubey, M. U. D. Rather, and A. Afroz, "Dynamical Analysis of Tumor-Dystrophin Interaction Model With Impact of Age of Onset and Staging," *Fixed Point Theory and Algorithms for Sciences and Engineering* 2025, no. 1 (2025): 4, https://doi.org/10.1186/s13663-025-00786-5.

[37] C. Mufudza, W. Sorofa, and E. T. Chiyaka, "Assessing the Effects of Estrogen on the Dynamics of Breast Cancer," *Computational and Mathematical Methods in Medicine* 2012 (2012): https://doi.org/10.1155/2012/473572.

[38] P. Van Den Driessche and J. Watmough, "Reproduction Numbers and Sub-Threshold Endemic Equilibria for Compartmental Models of Disease Transmission," *Mathematical Biosciences* 180, no. 1-2 (2002): 29–48, https://doi.org/10.1016/S0025-5564(02)00108-6.

[39] C. Castilo-Chavez, Z. Feng, and W. Haung, "On the Computation of R_0 and Its Role on Global Stability," in *Mathematical Approaches for Emerging and Reemerging Infectious Diseases: An Introduction* (Springer-Verlag, 2002), 229–250.

[40] L. S. Pontryagin, V. G. Boltyanskii, R. V. Gamkrelidze, and E. F. Mishchenko, *The Mathematical Theory of Optimal Processes* (Wiley Interscience, 1962).

[41] D. L. Luke, *Differential Equations: Classical to Controlled* (Academic Press, 1982).

[42] W. H. Fleming and R. W. Rishel, *Deterministic and Stochastic Optimal Control* (Springer-Verlag, 1975).

[43] S. I. Oke, M. B. Matadi, and S. Xulu, "Optimal Control Analysis of a Mathematical Model for Breast Cancer," *Mathematical and Computational Application* 23, no. 2 (2018): 21, https://doi.org/10.3390/mca2320021.

[44] J. C. Butcher, "A History of Runge-Kutta Methods," *Applied Numerical Mathematics* 20, no. 3 (1996): 247–260, https://doi.org/10.1016/0168-9274(95)00108-5.

[45] R. Fotouhi-C and W. Szyszkowski, "An Algorithm for Time-Optimal Control Problems," *Journal of Dynamic Systems, Measurement, and Control* 120, no. 3 (1998): 414–418, https://doi.org/10.1115/1.2805419.

[46] M. Itik, M. U. Salamci, and S. P. Banks, "SDRE Optimal Control of Drug Administration in Cancer Treatment," *Turkish Journal of Electrical Engineering and Computer Sciences* 18, no. 5 (2010): 715–730, https://doi.org/10.3906/elk-1001-411.

[47] R. Paul, A. Das, K. Dehingia, and H. K. Sarmah, "An Analysis of the Dynamics of a Cancerous Tumour Model With Targeted Chemotherapy," *Asian Journal of Pharmaceutical Research and Health* 12, no. 3 (2020): 130–140, https://doi.org/10.18311/ajprhc/2020/25431.

[48] R. Paul, A. Das, and H. K. Sarmah, "Global Stability Analysis to Control Growth of Tumor in an Immune-Tumournormal Cell Model With Drug Administration in the Form of Chemotherapy," *Indian Journal of Theoretical Physics* 65, no. 3-4 (2019): 92–107.

[49] D. S. Rodgrigues and P. D. Mancera, "Mathematical Analysis and Simulations Involving Chemotherapy and Surgery on Large Human Tumors Under a Suitable Cell-Kill Functional Response," *Mathematical Biosciences and Engineering* 10, no. 1 (2013): 221–234, https://doi.org/10.3934/mbe.2013.10.221.

[50] A. Saltelli, M. Ratto, T. Andres, et al., *Global Sensitivity Analysis: The Primer* (John Wiley & Sons, 2008).

[51] J. Savolainen, "Global Sensitivity Analysis of a Feedback-Controlled Stochastic Process Model," *Simulation Modelling Practice and Theory* 36 (2013): 1–10, https://doi.org/10.1016/j.simpat.2013.04.003.

[52] Q. W. Ren, Y. B. Chen, and X. J. Shu, "Global Sensitivity Analysis of Xinanjiang Model Parameters Based on Extend FAST Model," *Acta Scientiarum Naturalium Universitatis SunYatseni* 49, no. 3 (2010): 127–134.

[53] Y. Yang and H. Liu, "Sensitivity Analysis of Disease-Information Coupling Propagation Dynamics Model Parameters," *PLoS One* 17, no. 3 (2022): e0265273, https://doi.org/10.1371/journal.pone.0265273.

[54] S. Razavi and H. V. Gupta, "What Do We Mean By Sensitivity Analysis? The Need for Comprehensive Characterization of Global Sensitivity in Earth and Environmental Systems Models," *Water Resources Research* 51, no. 5 (2015): 3070–3092, https://doi.org/10.1002/2014WR016527.

[55] P. Rokforoz, A. A. Jamshidi, and N. N. Sarvestani, "Adaptive Robust Control of Cancer Chemotherapy With Extended Kalman Filter Observer," *Informatics in Medicine Unlocked* 8 (2017): 1–7, https://doi.org/10.1016/j.imu.2017.03.002.

[56] A. Ghaffari and N. Nasserifar, "Mathematical Modeling and Lyapunov-Based Drug Administration in Cancer Chemotherapy," *Iranian Journal of Electric Engineering* 5 (2009): 151–158.

[57] P. B. Borah, D. Robidas, K. Dehingia, B. J. Nath, and H. K. Sarmah, "On the Dynamics of COVID-19 Propagation With Vaccination and Optimal Control Strategies," *Brazilian Journal of Physics* 55, no. 3 (2025): 135, https://doi.org/10.1007/s13538-025-01769-y.

4185, 2025, 1, Downloaded from https://onlinelibrary.wiley.com/doi/10.1155/jama/5536333 by South African Medical Research, Wiley Online Library on [24/11/2025]. See the Terms and Conditions (https://onlinelibrary.wiley.com/terms-and-conditions) on Wiley Online Library for rules of use; OA articles are governed by the applicable Creative Commons License